

# SIP-BMM: Constructing Capability-Efficiency Pareto Set of LLMs via Bayesian Model Merging with Structural Importance Prior

Kesheng Chen, Yamin Hu, Zhenqian Zhu, Yiya Diao, Wenjian Luo

Guangdong Provincial Key Laboratory of Novel Security Intelligence Technologies,  
Institute of Cyberspace Security, College of Informatics,  
Harbin Institute of Technology, Shenzhen, China  
huyamin@hit.edu.cn

## Abstract

Navigating the capability-efficiency trade-offs in Large Language Models (LLMs) requires constructing a high-quality Pareto set. However, existing merging techniques remain inadequate: coarse-grained, model-level methods yield only a sparse set of suboptimal solutions, while fine-grained, layer-wise optimization suffers from the curse of dimensionality, especially under tight evaluation budgets where each model candidate is costly to assess. We propose Bayesian Model Merging with Structural Importance Prior (SIP-BMM), an evolutionary loop framework driven by Log-Noisy Expected Hypervolume Improvement ( $q$ NEHVI) that makes layer-wise Pareto set construction tractable by explicitly modeling which layers matter. Specifically, SIP-BMM derives a **Structural Importance Prior (SIP)** from layer-wise task-vector differences between base and expert models, and uses this prior to Bayesian Optimization toward a low effective dimensional subspace. Intuitively, SIP steers the optimizer to spend most trials on a small set of influential layers while largely ignoring layers that exhibit minimal task-relevant shifts. This importance-aware search preserves layer-wise control while substantially reducing sample complexity. Experiments show that SIP-BMM discovers a stronger and denser Pareto front than competitive baselines, enabling agile model selection under diverse operational constraints. Code is available at: <https://github.com/MiLab-HITSZ/2026-SIPBMM>.

## 1 Introduction

Large language models (LLMs) have revolutionized natural language processing by exhibiting remarkable reasoning abilities, often facilitated by chain-of-thought (CoT) prompting [Wei *et al.*, 2022]. However, extended reasoning sequences incur significant computational costs, including latency and token usage [Sui *et al.*, 2025]. In real deployments, these costs directly translate into throughput degradation and higher serving expense, motivating a careful balance between *capability* (e.g., reasoning ability) and *efficiency* (e.g., thinking token count). Model merging has therefore emerged as a

promising technique to amalgamate specialized models—for instance, by combining the weights of a reasoning-focused model and a non-reasoning base model through weighted averaging methods, thereby obtaining a merged model that balances reasoning capability and computational efficiency [Wu *et al.*, 2025; Team *et al.*, 2025].

Investigating the trade-offs between capability and efficiency enables LLMs to achieve optimal performance under varying scenario constraints or user preferences. Constructing a Pareto set of LLMs is essential for navigating these complex trade-offs. Nevertheless, prevalent merging techniques predominantly focus on coarse-grained, model-level merge, which we find yields only a limited number of solutions. This limitation stems from the fact that a single global interpolation weight cannot capture heterogeneous layer-wise specialization: different layers often contribute unevenly to reasoning, instruction following, and efficiency-related behaviors. As a result, model-level merging typically produces only a few discrete operating points and struggles to provide a continuous spectrum of capability–efficiency trade-offs, restricting flexibility in practical deployment. Moreover, these approaches often rely on manual hyperparameter tuning (e.g., sparsity thresholds or sign-agreement rules), making it difficult to systematically and reproducibly explore the trade-off landscape.

Conversely, recent layer-wise optimization methods attempt to increase granularity by searching for per-layer mixing coefficients using evolutionary computation or Bayesian optimization [Akiba *et al.*, 2025; Li *et al.*, 2025; Lee *et al.*, 2025]. While offering finer control, this strategy faces a critical scalability barrier as LLM depth increases: the decision space grows linearly with the number of layers, quickly reaching dozens (or more) of continuous dimensions. Under realistic evaluation budgets—where each candidate merge model must be validated on expensive benchmarks—this “curse of dimensionality” makes naive high-dimensional search sample-inefficient. In particular, surrogate-based optimization with standard Gaussian Processes (GPs) becomes computationally burdensome and statistically brittle in high dimensions, which can prevent the optimizer from reliably identifying a high-quality Pareto front.

To address these challenges, we propose SIP-BMM (**Bayesian Model Merging with Structural Importance Prior**) as shown in Figure 1, an automated evolutionary multi-

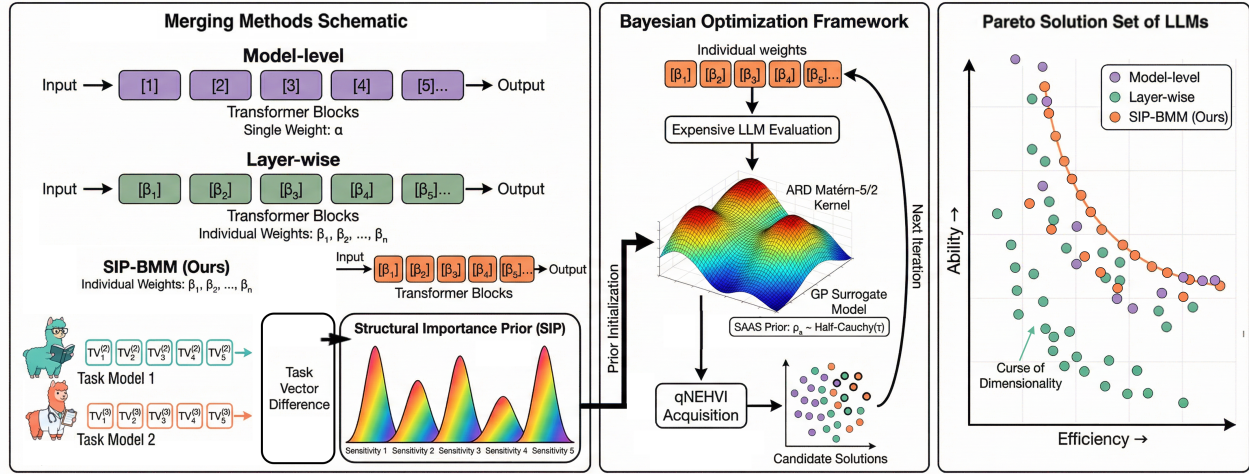


Figure 1: Schematic comparison of Pareto fronts constructed via different merging strategies. SIP-BMM leverages structural importance priors to efficiently navigate the high-dimensional layer-wise search space, achieving a denser and stronger front than coarse model-level and naive layer-wise approaches.

objective framework for constructing the LLM Pareto set via *layer-wise* merging. SIP-BMM injects architectural structure into the search by using a *Structural Importance Prior (SIP)*—computed from layer-wise task vector (TV) shifts between task models—to guide a Sparse Axis-Aligned Subspace Bayesian optimization (SAAS-BO) surrogate [Eriksson and Jankowiak, 2021]. This design biases the optimizer toward low effective dimensionality, enabling sample-efficient exploration in high-dimensional layer-wise spaces. To ensure stable and fair optimization across heterogeneous metrics, we further adopt a normalized objective formulation anchored by established base and expert models. The overall process is driven by the  $q$ -Log Noisy Expected Hypervolume Improvement (qNEHVI) acquisition function [Daulton *et al.*, 2020] to efficiently refine and diversify the Pareto frontier under limited evaluation budgets. Experiments show that SIP-BMM discovers a stronger and denser Pareto front than competitive model-level merging baselines, enabling rapid model selection under diverse operational constraints.

**Contributions.** Our contributions are as follows:

We provide experimental evidence that model-level coarse-grained merging is insufficient for fully exploring the Pareto frontier. Only layer-wise optimization can unlock the full capability–efficiency trade-off spectrum, as coarse-grained strategies fail to express the heterogeneous weight structures required for optimal mid-front solutions.

We present SIP-BMM, the first automated evolutionary multi-objective framework for constructing the capability–efficiency Pareto frontier via LLM merging. Under matched evaluation budgets, SIP-BMM discovers a denser and stronger Pareto front (higher hypervolume and coverage) than all model-level merging baselines.

We propose a Structural Importance Prior (SIP) that leverages layer-wise task-vector differences to guide Bayesian optimization. By converting architectural sensitivity into lengthscale priors, SIP enables effective warm-starting and focused exploration in high-dimensional spaces.

## 2 Background

### 2.1 Model Merging Methods

Model merging combines the parameters of multiple neural networks into a unified model  $\mathcal{M}_{\text{merge}}$  to amalgamate complementary capabilities without retraining from scratch [Yang *et al.*, 2024]. Given a set of  $K$  models  $\{\mathcal{M}^{(1)}, \dots, \mathcal{M}^{(K)}\}$  derived from a common base model  $\mathcal{M}_{\text{base}}$ , the objective is to find an effective merge of their task vectors or weights.

Early parameter-level strategies focus on mitigating interference during merge. Weight averaging [Utans, 1996] and task arithmetic [Ilharco *et al.*, 2022] provide basic interpolation and vector manipulation. More advanced methods like TIES-Merging [Yadav *et al.*, 2023], DARE-Merging [Yu *et al.*, 2024], and DELLA-Merging [Deep *et al.*, 2024] introduce sparsification, sign agreement, and pruning to reduce redundancy and conflicts. While computationally efficient, these methods predominantly operate at a coarse, model-level granularity and often rely on handcrafted hyperparameters, making them insufficient for systematically exploring the LLM capability–efficiency trade-off surface.

In pursuit of automating the merging process, evolutionary computation-based methods have recently emerged. TIES-DARE [Akiba *et al.*, 2025] utilizes CMA-ES [Hansen *et al.*, 2003] to search for layer-wise mixing coefficients, though it primarily focuses on single-objective optimization. However, since this algorithm employs a single-objective evolutionary approach, it requires a substantial evaluation budget and is unsuitable for multi-objective optimization scenarios such as LLM-PF construction. MO-MM [Li *et al.*, 2025] formulates merging as a multi-objective problem, employing Bayesian optimization with the Log-Noisy Expected Hypervolume Improvement ( $q$ NEHVI) acquisition function [Daulton *et al.*, 2020] to identify Pareto-optimal solutions across conflicting tasks. However, as LLM depth increases, these layer-wise approaches encounter the curse of dimensionality: the resulting high-dimensional search space renders standard Gaussian Process surrogates computationally intractable and prone to

overfitting [Eriksson and Jankowiak, 2021]. This motivates our framework that maintains fine-grained control while exploiting structural priors to navigate high-dimensional spaces efficiently.

## 2.2 Multiobjective Optimization

Multi-objective optimization (MO) aims to find a set of solutions that represent optimal trade-offs among conflicting objectives [Deb *et al.*, 2002]. The central concept is the Pareto front: solutions for which no objective can be improved without degrading at least one other objective. A multi-objective optimization problem (MOP) is commonly stated as optimizing a vector of objective functions

$$F(\mathbf{x}) = (f_1(\mathbf{x}), f_2(\mathbf{x}), \dots, f_m(\mathbf{x})),$$

subject to constraints, where  $X$  is a decision vector in the feasible region. Key concepts include:

- **Pareto dominance:**  $\mathbf{x}$  dominates  $\mathbf{Y}$  if  $f_i(\mathbf{x}) \leq f_i(\mathbf{Y})$  for all  $i$  and  $f_j(\mathbf{x}) < f_j(\mathbf{y})$  for at least one  $j$  (for minimization; inequalities reverse for maximization).
- **Pareto optimality:** a solution is Pareto optimal if no other feasible solution dominates it.
- **Pareto set (PS):** the set of all Pareto-optimal solutions in decision space.
- **Pareto front (PF):** the image of the PS in objective space, representing the optimal trade-offs.

## 3 Methodology

### 3.1 Problem Formulation

Our goal is to construct an LLM Pareto set that captures trade-offs between reasoning capability and efficiency, enabling rapid deployment of models under different operational constraints without retraining. The Pareto set can further be combined with routing strategies or user preferences to select an appropriate model for a given scenario.

**Multi-objective model merge.** We formulate model merge as a multi-objective optimization problem with  $K$  objectives:

$$\max F(\mathcal{M}_{\text{merge}}) = (f_1(\mathcal{M}_{\text{merge}}), \dots, f_K(\mathcal{M}_{\text{merge}})), \quad (1)$$

where  $f_k$  denotes the  $k$ -th capability-related objective.

**Normalized Objectives.** To ensure fairness across different benchmarks and prevent the algorithm from over-preferring a single benchmark, we normalize the objective functions. Although this normalization does not guarantee that all objective values fall within the  $[0, 1]$  range, it effectively balances the influence of heterogeneous benchmarks in multi-objective optimization.

Formally, the benchmark set for the  $k$ -th capability is denoted as  $Q^{(k)} = \{q_1^{(k)}, q_2^{(k)}, \dots, q_N^{(k)}\}$ , where  $q_n^{(k)}$  represents the  $n$ -th benchmark. The corresponding metric evaluation functions are defined as  $S^{(k)} = \{s_1^{(k)}(\cdot), \dots, s_N^{(k)}(\cdot)\}$ , where  $s_n^{(k)}(\mathcal{M}_{\text{merge}})$  evaluates the merged model  $\mathcal{M}_{\text{merge}}$  on benchmark  $q_n^{(k)}$ .

Let  $\mathcal{M}_{\text{expert}}^{(k)}$  be the expert model specialized for the  $k$ -th capability, and  $\mathcal{M}_{\text{vanilla}}^{(k)}$  be the corresponding vanilla reference model. Note that we intentionally designate the worst-performing model as the vanilla reference during normalization to avoid confusion with the term “base model,” which is commonly used in model merging literature. Based on these definitions, the normalized objective for the  $k$ -th capability is computed as:

$$f_k(\mathcal{M}_{\text{merge}}) = \sum_{s^{(k)} \in S^{(k)}} \left( \frac{s^{(k)}(\mathcal{M}_{\text{merge}}) - s^{(k)}(\mathcal{M}_{\text{vanilla}}^{(k)})}{s^{(k)}(\mathcal{M}_{\text{expert}}^{(k)}) - s^{(k)}(\mathcal{M}_{\text{vanilla}}^{(k)})} \cdot \frac{1}{N} \right). \quad (2)$$

**Task vector extraction.** Most existing LLM merging methods follow a common recipe: given a task-specific model and the base model, first compute a corresponding task vector, and then obtain the merged model by applying arithmetic operations [Yadav *et al.*, 2023; Davari and Belilovsky, 2024] to the base model and the task vectors (TVs).

We refine this operation to the layer-wise, for the  $i$ -th task model  $\mathcal{M}^{(i)}$  and the base model  $\mathcal{M}_{\text{base}}$ , we can extract layer-wise task vectors  $TV_{i,l}$ :

$$TV_{i,l} = \mathcal{M}_{i,l} - \mathcal{M}_{\text{base},l}, \quad l = 1, \dots, L, \quad (3)$$

where  $\mathcal{M}_{\text{merge},l}$  and  $\mathcal{M}_{i,l}$  represent the parameters of merge model and the  $i$ -th task model at layer  $l$ ,  $TV_{i,l}$  represent the parameters of task vector for the  $i$ -th task model at layer  $l$ .

Model-level merge methods directly apply the task vector to the base model  $\mathcal{M}_{\text{merge},l} = \mathcal{M}_{\text{base},l} + \alpha \sum_{i=1}^T \Theta(TV_{i,l})$ , which use the same weight  $\alpha$  for all layer  $l$ . Whereas methods such as TIES [Yadav *et al.*, 2023], DARE [Yu *et al.*, 2024] perform operations like trimming and rescaling on the set of task vectors before combining them with the base model. We abstract these method-specific transformations as  $\Theta(TV_{i,l})$ . Specifically, task arithmetic (TA) use identity transformation.

**Layer-wise merging parameterization.** To achieve fine-grained control over behavior, we perform interpolation at the layer level, assigning independent weights to each Transformer layer. Let the decision vector be  $\mathbf{x} \in [0, 1]^D$  with  $D = L$  (one scalar per layer). For the two-model case,  $\mathbf{x}$  directly specifies the layer-wise interpolation weights; for the multi-expert case,  $\mathbf{x}$  can be mapped to simplex weights by a normalization operator. Concretely, we write:

$$\begin{aligned} \mathcal{M}_{\text{merge}} &= \text{Layer-Wise-Merge}(\{\mathcal{M}_{i,l}\}; \mathbf{x}), \\ \mathbf{x} &= (x_1, \dots, x_L), i \in T, x_l \in [0, 1], l = 1, \dots, L, \end{aligned} \quad (4)$$

where  $T$  is the task model set. In the two-model interpolation [Wu *et al.*, 2025] scenario, the merged weight for layer  $l$  is computed as a convex combination:  $\mathcal{M}_{\text{merge},l} = \mathcal{M}_{\text{base},l} + x_l \cdot TV_{1,l} + (1 - x_l) \cdot TV_{2,l}$ .

### 3.2 Structural Importance Prior

To scale optimization to the full layer-wise search space while maintaining sample efficiency, we propose an *Structural Importance Prior* strategy.

**Functional difference quantification.** Here, we propose a method-agnostic quantification tailored to this family of merging approaches: we measure the *layer-wise disagreement* under a given merging algorithm by computing the dispersion (variance-like deviation) of the processed task vectors. Without loss of generality, we quantify the disagreement at the  $l$ -th Transformer block using the  $\ell_p$ -norm.

We compute the layer-wise difference  $\text{Diff}_l$  to measure functional divergence of each layer across specialized models:

$$\text{Diff}_l = \sum_{i=1}^N \left\| \Theta(TV_{i,l}) - \frac{1}{N} \sum_{j=1}^N \Theta(TV_{j,l}) \right\|_p. \quad (5)$$

In particular, when the merging method is task arithmetic,  $\Theta$  reduces to the identity mapping.

**Sensitivity mapping.** After computing the disagreement score for the  $l$ -th Transformer block, we leverage the intuition that layers with larger disagreement tend to have a more significant impact on the merging outcome. Therefore, we use this disagreement prior to initialize the lengthscales of different dimensions in the ARD kernel, making the surrogate more sensitive to layers with higher disagreement.

Concretely, we use min-max normalization to normalize differences into an importance score  $\mathcal{I}_d = \text{Norm}(\text{Diff}_d) \in [0, 1]$  and map  $\mathcal{I}_d$  to initial lengthscales  $\ell_d^{(0)}$  via a piecewise function  $\Phi$ :

$$\ell_d^{(0)} = \Phi(\mathcal{I}_d) = \begin{cases} 0.5, & \text{if } \mathcal{I}_d > 0.9 \text{ (Critical)} \\ 1.0, & \text{if } 0.8 < \mathcal{I}_d \leq 0.9 \text{ (Important)} \\ 5.0, & \text{if } \mathcal{I}_d \leq 0.7 \text{ (Stable)} \end{cases}. \quad (6)$$

**SAAS GP surrogate.** Following [Williams and Rasmussen, 2006], we use an ARD Matérn-5/2 kernel to model each objective:

$$k(\mathbf{x}, \mathbf{x}') = \sigma_f^2 \left( 1 + \sqrt{5}r + \frac{5}{3}r^2 \right) \exp(-\sqrt{5}r), \quad (7)$$

where  $r = \sqrt{\sum_{d=1}^D \frac{(x_d - x'_d)^2}{\ell_d^2}}$ , to enforce sparsity in high dimensions, we adopt the hierarchical SAAS prior [Eriksson and Jankowiak, 2021] on inverse squared lengthscales  $\rho_d = 1/\ell_d^2$ . By initializing the NUTS sampler [Hoffman and Gelman, 2014] with SIP-derived  $\ell_d^{(0)}$ , we warm-start exploration in architecturally significant regions.

### 3.3 Optimization Framework

**Bayesian optimization loop.** We optimize in the decision space  $\mathbf{x} \in [0, 1]^D$ , where each  $\mathbf{x}$  defines a merged model  $\mathcal{M}_{\text{merge}}(\mathbf{x})$  (Eq. (4)) and an objective vector  $\mathbf{y}(\mathbf{x}) = (y_1(\mathbf{x}), \dots, y_K(\mathbf{x}))$  with  $y_k(\mathbf{x}) = f_k(\mathcal{M}_{\text{merge}}(\mathbf{x}))$  (Eq. (2)).

At iteration  $t$ , we fit a multi-output surrogate (implemented as  $K$  independent SAAS GPs for simplicity) on  $\mathcal{D}_t = \{(\mathbf{x}_i, \mathbf{y}_i)\}_{i=1}^{n_t}$ . We then select a batch of  $q$  candidates by maximizing the Log-Noisy Expected Hypervolume Improvement ( $q$ NEHVI) acquisition function [Daulton *et al.*, 2022].

**$q$ NEHVI.** We adopt the  $q$ NEHVI acquisition function from prior work [Daulton *et al.*, 2022]. Let  $\mathcal{P}_t$  be the observed nondominated set and  $\mathbf{r} \in \mathbb{R}^K$  a reference point. For  $q$  new objective vectors  $\mathbf{Y}$ , the hypervolume improvement (HVI) is

$$\text{HVI}(\mathbf{Y}; \mathcal{P}_t, \mathbf{r}) = \text{HV}(\mathcal{P}_t \cup \mathbf{Y}; \mathbf{r}) - \text{HV}(\mathcal{P}_t; \mathbf{r}). \quad (8)$$

We estimate and optimize  $\alpha_{q\text{NEHVI}}$  via Monte-Carlo sampling with the log-stabilized implementation of [Daulton *et al.*, 2022]. Further implementation details are provided in supplementary material.

**Solution selection.** After obtaining the LLM Pareto set, we compute cosine similarity between normalized objective vectors  $\mathcal{Y}_P$  of Pareto solutions and a user-defined preference vector, then select the best overall model from the Top- $K$  solutions with the highest cosine similarity. The overall optimization process is summarized in Algorithm 1.

---

#### Algorithm 1 The SIP-BMM Optimization Framework

---

**Input:** Expert models  $\{\mathcal{M}_{\text{expert}}^{(k)}\}$ , Vanilla models  $\{\mathcal{M}_{\text{vanilla}}^{(k)}\}$ , initial points  $\mathcal{N}_0$ , iterations  $T$ , batch size  $q$   
**Output:** Final Pareto set  $\mathcal{X}_{\text{final}}$  and Pareto front  $\mathcal{Y}_{\text{final}}$

// 1. *Prior Extraction*  
Compute  $\text{Diff}_l$  for all layers  $l \in \{1, \dots, L\}$  using Eq. (5)  
Initialize SIP lengthscales  $\ell_d^{(0)} \leftarrow \Phi(\text{Norm}(\text{Diff}_d))$  using Eq. (6)

// 2. *Initialization*  
 $\mathcal{X}_0 \leftarrow \text{SobolSamples}(\mathcal{N}_0)$   
 $\mathcal{Y}_0 \leftarrow \text{EvaluateObjectives}(\mathcal{X}_0, \{\mathcal{M}_{\text{expert}}^{(k)}\}, \{\mathcal{M}_{\text{vanilla}}^{(k)}\})$

// 3. *BO with Structural Importance Prior Loop*  
**for**  $t = 0$  **to**  $T - 1$  **do**  
Fit SAAS GP with SIP:  $GP_t \leftarrow \text{FitSAAS}(\mathcal{X}_t, \mathcal{Y}_t, \ell_d^{(0)})$   
 $\mathcal{X}_{\text{new}} \leftarrow \text{OptimizeAcquisition}(q\text{NEHVI}, GP_t, q)$   
 $\mathcal{Y}_{\text{new}} \leftarrow \text{EvaluateObjectives}(\mathcal{X}_{\text{new}})$   
 $\mathcal{X}_{t+1} \leftarrow \mathcal{X}_t \cup \mathcal{X}_{\text{new}}; \mathcal{Y}_{t+1} \leftarrow \mathcal{Y}_t \cup \mathcal{Y}_{\text{new}}$   
**end for**  
 $(\mathcal{X}_P, \mathcal{Y}_P) \leftarrow \text{GetParetoFront}(\mathcal{X}_T, \mathcal{Y}_T)$   
 $(\mathcal{X}_{\text{final}}, \mathcal{Y}_{\text{final}}) \leftarrow \text{SelectSolution}(\mathcal{X}_P, \mathcal{Y}_P)$

---

## 4 Experimental Setup

### 4.1 Models and Benchmarks

We formulate the optimization problem with two conflicting objectives: reasoning capability  $f_{\text{reasoning}}$  and model efficiency  $f_{\text{efficiency}}$ . Our goal is to simultaneously improve reasoning performance and computational efficiency by fusing a specialized “Thinking” model  $\mathcal{M}_{\text{think}}$  with an efficiency-oriented “Instruct” model  $\mathcal{M}_{\text{instruct}}$ .

We employ rigorous benchmarks including GPQA-Diamond [Rein *et al.*, 2024] and AIME25. The specific model parameter settings and definitions are summarized in Table 1. We select the post-trained thinking model (the Thinking Model, Qwen3-4B-Thinking [Yang *et al.*, 2025]) as the reasoning expert. Reasoning is assessed using GPQA-Diamond and AIME25, with mean accuracy as the metric. We select the post-trained instruct model (the Instruct Model,

Table 1: Multi-objective Model Interpolation Parameter Settings

Parameter	Setting
Objective 1 (Eq. (2))	$f_1 = \text{Reasoning}$
Expert Model for $f_1$ (Eq. (2))	$\mathcal{M}_{\text{expert}}^{(1)} = \text{Thinking Model}$
Vanilla Model for $f_1$ (Eq. (2))	$\mathcal{M}_{\text{vanilla}}^{(1)} = \text{Instruct Model}$
Metric evaluation function for $f_1$	$M^{(1)} = \{\text{Mean Acc., Mean Acc.}\}$
Benchmarks for $f_1$	$Q^{(1)} = \{\text{GPQA-Diamond, AIME25}\}$
Objective 2 (Eq. (2))	$f_2 = \text{Efficiency}$
Expert Model for $f_2$ (Eq. (2))	$\mathcal{M}_{\text{expert}}^{(2)} = \text{Instruct Model}$
Vanilla Model for $f_2$ (Eq. (2))	$\mathcal{M}_{\text{vanilla}}^{(2)} = \text{Thinking Model}$
Metric evaluation function for $f_2$	$M^{(2)} = \{\text{Mean Token Count., Mean Token Count}\}$
Benchmarks for $f_2$	$Q^{(2)} = \{\text{GPQA-Diamond, AIME25}\}$
Task Model (Eq. (4))	$\mathcal{M}_1 = \text{Thinking Model}, \mathcal{M}_2 = \text{Instruct Model}$
Base Model (Eq. (4))	$\mathcal{M}_{\text{base}} = \text{Instruct Model}$

Qwen3-4B-Instruct [Yang *et al.*, 2025]) as the efficiency expert, with mean output token count as the metric.

For objective normalization, we set the “vanilla” reference for each objective to be the opposing expert model (e.g., Instruct model serves as the vanilla model for reasoning, and thinking model serves as the vanilla model for efficiency).

## 4.2 Baselines

We evaluate SIP-BMM against five typical model-level merging methods: (1) Task Arithmetic [Ilharco *et al.*, 2022]; (2) TIES-Merging [Yadav *et al.*, 2023]; (3) DARE-Merging [Yu *et al.*, 2024]; (4) Breadcrumbs [Davari and Belilovsky, 2024]; and (5) DELLA [Deep *et al.*, 2024]. (6) SASS-BO, a variant similar to MO-MM [Li *et al.*, 2025] but without the differential evolution (DE) operator.

## 4.3 Experimental Settings

**Granularity comparison.** To verify the necessity of layer-wise optimization, we construct solution sets using varying granularities: (1) model-level (a single global weight); (2) block-wise ( $n = 9$ ) and block-wise( $n = 9$ ), where  $n$  is the blocks num; and (3) layer-wise (independent weights for all 36 layers). For block-wise merging, we partition layers into  $K$  blocks using a *hybrid* Fisher-Jenks-style dynamic programming algorithm based on layer-wise task-vector difference magnitudes: it jointly encourages within-block homogeneity (variance) while balancing the total “difference mass” across blocks (sum deviation), so that highly active deep layers can be isolated instead of being diluted by many stable shallow layers. Full formulation and implementation details are provided in supplementary material.

**Baseline Comparison** We compare SIP-BMM against five model-level merging methods: Task Arithmetic (TA), TIES, DARE, Breadcrumbs, and DELLA. For SIP-BMM, we use  $N_0 = 8$  initial samples and run  $T = 20$  iterations with batch size  $q = 4$ . All baselines share the same evaluation budget  $B = 88$  real evaluations. Under this budget, model-level baselines are executed via adaptive grid search: for TA, we grid-search  $\lambda \in [0.05, 0.95]$ ; for methods with an additional density hyperparameter  $\delta \in [0.7, 0.9]$ , we jointly grid-search  $\lambda$  and  $\delta$  using a 9:2 grid-point allocation based on interval lengths. All evaluations are performed exhaustively until the budget is consumed.

Table 2: Summary metrics across different merging granularities.

GRANULARITY	HV VALUE	COVERAGE	PARETO #
LAYER-WISE	1.322373	<b>9/13</b>	<b>10</b>
BLOCK-WISE ( $n=18$ )	<b>1.364006</b>	1/13	9
BLOCK-WISE ( $n=9$ )	1.290996	0/13	14
MODEL-LEVEL	1.270630	3/13	13

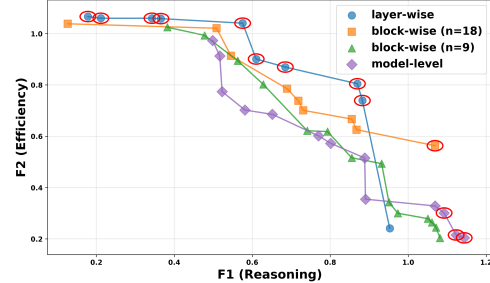


Figure 2: Distribution of merged models in objective space.

**Ablation study.** To isolate the contribution of the Structural Importance Prior (SIP), we compare: (1) SIP-BMM (BO + SAAS + SIP) and (2) vanilla SAAS-BO (BO + SAAS and without SIP initialization). All configurations use the same evaluation budget.

For all above experiments, inference parameters follow the official recommended settings for Qwen3 [Yang *et al.*, 2025], and all optimization runs use a fixed seed for reproducibility.

## 5 Results and Analysis

### 5.1 The Necessity of Layer-wise Granularity

Figure 2 and Table 2 illustrate Pareto fronts and summary metrics obtained with different merging granularities, ranging from model-level grid search to block-wise and finally to full layer-wise optimization. We observe a consistent trend: as the number of independent weight parameters increases, the Pareto front shifts toward improved trade-offs, indicating gains in both reasoning capability and token efficiency.

In Table 2, where **Coverage** metric mean the proportion of the Pareto set (PS) contributed by this algorithm out of the PS formed jointly by all algorithms, **Pareto** metric mean the number of solutions in the algorithm’s PS. the layer-wise approach achieves the highest coverage (9/13), indicating a superior approximation of the optimal trade-off surface. This result suggests that LLM capabilities are distributed heterogeneously across layers: while hard block partitioning reduces dimensionality, it can obscure fine-grained, layer-specific contributions that are critical for capturing nuanced trade-offs. These findings motivate scaling optimization to the full layer-wise space using SIP-BMM. Detailed metrics are provided in the supplementary material.

**Why finer granularity matters.** Beyond the overall improvement, Figure 2 reveals a consistent pattern: increasing the optimization granularity yields the largest gains in the *intermediate* region of the Pareto front, while differences near the two extremes remain comparatively small. A plausible explanation is that extreme solutions are often dominated by candidates with nearly degenerate merge patterns (e.g.,  $\lambda \approx 0$

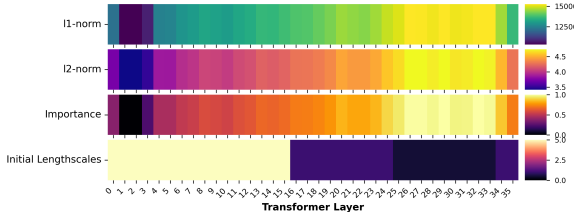


Figure 3: Visualization of the Structural Importance Prior (SIP).

Table 3: SIP-BMM against baseline merging methods.

METHOD	HV VALUE	COVERAGE	PARETO #
SIP-BMM (OURS)	<b>1.397793</b>	<b>14/22</b>	<b>17</b>
BREADCRUMBS	0.566634	1/22	2
TA	1.270630	3/22	13
DARE	1.257203	0/22	11
DELLA	1.301842	4/22	11
TIES	0.368805	0/22	5

or  $\lambda \approx 1$ , or layer weights concentrated near 0 or 1), which effectively collapse to “almost-efficiency” or “almost-ability” models. Such solutions exhibit low-complexity weight structures and can therefore be approximated reasonably well even with coarse model-level or block-wise parameterizations. In contrast, mid-front solutions typically require heterogeneous, layer-dependent combinations to simultaneously balance capability and efficiency. These higher-complexity compositions cannot be expressed by coarse-grained merging strategies, explaining why finer (ideally layer-wise) granularity is essential for uncovering the true Pareto frontier.

**Critical Observation:** Searching for model-level merge weights, even with fine-grained grid search, is insufficient to uncover the true Pareto frontier obtainable through model merging. Fine-grained weight parameterization—particularly **layer-wise strategies**—is essential for fully exploiting the capability–efficiency trade-off space.

## 5.2 Main Results

### Structural Importance Prior Visualization

Before presenting the baseline comparison, we visualize the extracted Structural Importance Prior (SIP) that guides the high-dimensional layer-wise search in SIP-BMM.

Figure 3 summarizes, across Transformer layers, (i) L1-norm differences of task vectors, (ii) L2-norm differences, (iii) normalized differences used to produce importance scores, and (iv) the resulting lengthscale prior parameters used to initialize the SAAS-GP surrogate. The sensitivity is highly non-uniform across layers, motivating an importance-aware subspace Bayesian optimization strategy.

### Main Results: SIP-BMM vs. Baselines

Table 3, 4 and Figure 4 present the performance of SIP-BMM compared to model-level merging methods. SIP-BMM consistently discovers a stronger and denser Pareto front. While model-level baselines like Task Arithmetic and Breadcrumbs provide a few competitive points, they fail to explore the continuous spectrum of trade-offs.

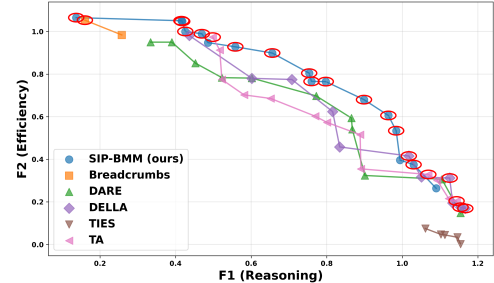


Figure 4: Distribution of merged models in objective space.

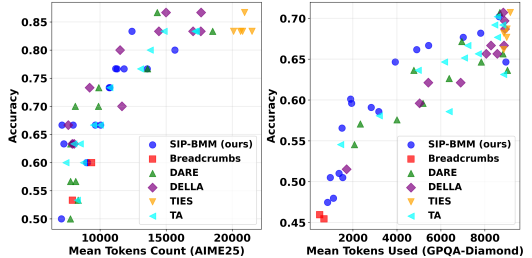


Figure 5: Pareto front on benchmarks (Tokens vs. Accuracy).

SIP-BMM leverages the flexibility of layer-wise weights to find “sweet spots” where reasoning accuracy is maintained with significantly lower token counts. The hypervolume (HV) for SIP-BMM exceeds the best-performing baseline, demonstrating its effectiveness in navigating complex objective spaces. To further understand performance on specific tasks, Figure 5 show trade-offs between accuracy and token efficiency on each benchmark. The results demonstrate that the performance improvement achieved by SIP-BMM relies on enhancements across all benchmarks rather than a single one, which aligns with the motivation behind our design of the normalized objective function.

### 5.3 Ablation Study: Impact of SIP

To dissect the factors contributing to SIP-BMM’s performance, we study the impact of SIP through ablations in the following section. Table 5 and Figure 6 present the performance of SIP-BMM compared to the same framework without SIP (BMM). While vanilla SAAS-BO can eventually identify relevant dimensions, SIP-BMM achieves higher HV and coverage under the same evaluation budget. This indicates SIP provides an effective warm-start, allowing the sampler to focus on critical layers earlier. The results support that integrating architectural priors (SIP) with subspace optimization (SAAS-BO) is crucial.

### 5.4 Solution Analysis

To demonstrate this customization capability in the solution selection phase, we simulate user preferences by sampling preference vectors from a uniform distribution over the trade-off space. As shown in the Figure 7, the resulting Pareto set is both dense and diverse, providing good coverage across different capability–efficiency regimes and thus reliably satisfying heterogeneous preference distributions (including the uniformly distributed one used here) with minimal additional search. The detailed benchmark results are provided in the supplementary material.

Table 4: Detailed performance comparison of individual candidates across all methods.

ID	Method	$f_1 (\uparrow)$	$f_2 (\uparrow)$	Acc. <sup>1</sup> (%)	Token count <sup>1</sup> (#)	Acc. <sup>2</sup> (%)	Token count <sup>2</sup> (#)	Pareto
0		1.0301	0.3747	64.65	8,952	83.34	12,417	✓
1		0.4175	1.0474	47.98	1,116	66.66	7,120	✓
2		0.7597	0.7656	64.65	3,927	66.67	10,038	✓
3		0.6560	0.8988	59.60	1,937	66.66	9,638	✓
4		0.7976	0.7646	58.59	3,174	76.67	11,178	✓
5		0.4858	0.9476	56.57	1,503	60.00	9,053	✗
6		0.7537	0.8042	59.09	2,830	73.33	10,691	✓
7		0.9632	0.6057	66.67	5,440	76.66	11,815	✓
8	SIP-BMM (ours)	0.4155	1.0504	50.51	973	63.33	7,256	✓
9		0.4695	0.9892	50.51	1,535	66.66	7,961	✓
10		0.5582	0.9280	60.10	1,894	60.00	8,968	✓
11		1.0898	0.2636	70.20	8,650	80.00	15,657	✗
12		0.1369	1.0650	47.47	848	50.00	7,073	✓
13		0.9839	0.5339	67.68	7,015	76.66	11,286	✓
14		0.8987	0.6799	66.16	4,902	73.33	10,748	✓
15		0.4257	0.9999	51.01	1,368	63.33	7,939	✓
16		0.9942	0.3963	68.18	7,808	76.66	13,571	✗
0	Breadcrumbs	0.1599	1.0530	45.96	490	53.33	7,906	✓
1		0.2576	0.9837	45.45	686	60.00	9,357	✗
0–10	DARE	All candidates are non-Pareto (dominated).						✗
1		1.0174	0.4153	66.67	8,872	80.00	11,517	✓
2	DELLA (Pareto points)	1.1255	0.3119	66.67	8,277	86.67	14,996	✓
4		1.1544	0.1745	70.71	8,834	83.34	17,624	✓
10		1.1670	0.1690	68.69	8,913	86.67	17,647	✓
0,3,5–9	DELLA (others)	Non-Pareto points omitted for brevity.						✗
0–4	TIES	All candidates are non-Pareto (dominated).						✗
0		0.4983	0.9734	54.55	1,441	63.33	8,496	✓
9	TA (Pareto points)	1.0691	0.3285	69.19	8,812	80.00	13,786	✓
12		1.1438	0.2042	70.20	8,560	83.33	17,285	✓
1–8,10–11	TA (others)	Non-Pareto points omitted for brevity.						✗

<sup>1</sup> Metrics evaluated on the GPQA-Diamond dataset. <sup>2</sup> Metrics evaluated on the AIME25 dataset.

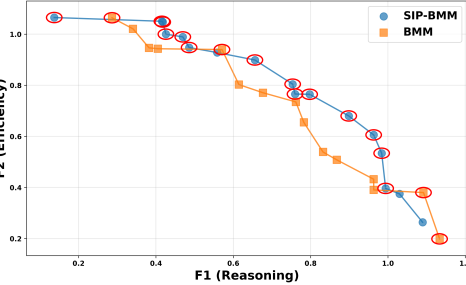


Figure 6: Ablation study results in objective space.

Table 5: Ablation study: Impact of SIP prior.

METHOD	HV VALUE	COVERAGE	PARETO #
SIP-BMM (OURS)	<b>1.397793</b>	<b>14/18</b>	<b>17</b>
SAAS-BO	1.358740	4/18	15

## 6 Conclusion

We introduced SIP-BMM, a framework for constructing LLM Pareto sets by integrating Structural Importance Priors (SIP) with SAAS-BO. We studied the fundamental trade-off between reasoning capability and efficiency, showing that coarse model-level merging is insufficient, while naive layer-

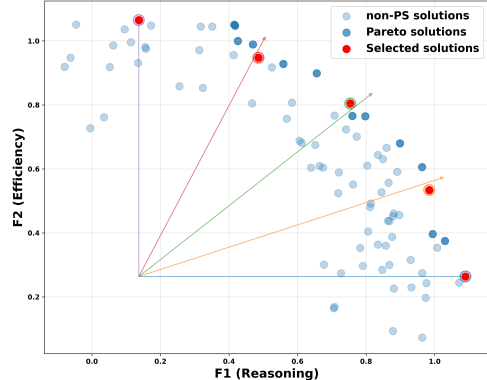


Figure 7: Visualization of Pareto-optimal and dominated solutions.

wise optimization is hindered by the curse of dimensionality. By leveraging task-vector differences to quantify layer sensitivity, SIP-BMM identifies critical layers and guides the search within a sparse axis-aligned subspace, making fine-grained high-dimensional optimization feasible under strict evaluation budgets. Experiments demonstrate that SIP-BMM produces stronger and denser Pareto fronts with improved hypervolume.

## Ethical Statement

There are no ethical issues.

## References

[Akiba *et al.*, 2025] Takuya Akiba, Makoto Shing, Yujin Tang, Qi Sun, and David Ha. Evolutionary optimization of model merging recipes. *Nature Machine Intelligence*, 7(2):195–204, 2025.

[Daulton *et al.*, 2020] Samuel Daulton, Maximilian Balandat, and Eytan Bakshy. Differentiable expected hyper-volume improvement for parallel multi-objective bayesian optimization. *Advances in neural information processing systems*, 33:9851–9864, 2020.

[Daulton *et al.*, 2022] Samuel Daulton, Sait Cakmak, Maximilian Balandat, Michael A Osborne, Enlu Zhou, and Eytan Bakshy. Robust multi-objective bayesian optimization under input noise. In *International Conference on Machine Learning*, pages 4831–4866. PMLR, 2022.

[Davari and Belilovsky, 2024] MohammadReza Davari and Eugene Belilovsky. Model breadcrumbs: Scaling multi-task model merging with sparse masks. In *European Conference on Computer Vision*, pages 270–287. Springer, 2024.

[Deb *et al.*, 2002] Kalyanmoy Deb, Amrit Pratap, Sameer Agarwal, and TAMT Meyarivan. A fast and elitist multi-objective genetic algorithm: NSGA-II. *IEEE transactions on evolutionary computation*, 6(2):182–197, 2002.

[Deep *et al.*, 2024] Pala Tej Deep, Rishabh Bhardwaj, and Soujanya Poria. Delta-merging: Reducing interference in model merging through magnitude-based sampling. *arXiv preprint arXiv:2406.11617*, 2024.

[Eriksson and Jankowiak, 2021] David Eriksson and Martin Jankowiak. High-dimensional bayesian optimization with sparse axis-aligned subspaces. In *Proceedings of the Thirty-Seventh Conference on Uncertainty in Artificial Intelligence*, pages 493–503. PMLR, 2021.

[Hansen *et al.*, 2003] Nikolaus Hansen, Sibylle D Müller, and Petros Koumoutsakos. Reducing the time complexity of the derandomized evolution strategy with covariance matrix adaptation (CMA-ES). *Evolutionary computation*, 11(1):1–18, 2003.

[Hoffman and Gelman, 2014] Matthew D Hoffman and Andrew Gelman. The No-U-Turn sampler: adaptively setting path lengths in hamiltonian monte carlo. *Journal of Machine Learning Research*, 15(1):1593–1623, 2014.

[Ilharco *et al.*, 2022] Gabriel Ilharco, Marco Túlio Ribeiro, Mitchell Wortsman, Suchin Gururangan, Ludwig Schmidt, Hannaneh Hajishirzi, and Ali Farhadi. Editing models with task arithmetic. *arXiv preprint arXiv:2212.04089*, 2022.

[Lee *et al.*, 2025] Sanwoo Lee, Jiahao Liu, Qifan Wang, Jingga Wang, Xunliang Cai, and Yunfang Wu. Dynamic fisher-weighted model merging via bayesian optimization. *arXiv preprint arXiv:2504.18992*, 2025.

[Li *et al.*, 2025] Bingdong Li, Zixiang Di, Yanting Yang, Hong Qian, Peng Yang, Hao Hao, Ke Tang, and Aimin Zhou. It’s morphing time: Unleashing the potential of multiple llms via multi-objective optimization. *IEEE Transactions on Evolutionary Computation*, 2025.

[Rein *et al.*, 2024] David Rein, Betty Li Hou, Asa Cooper Stickland, Jackson Petty, Richard Yuanzhe Pang, Julien Dirani, Julian Michael, and Samuel R Bowman. Gpqa: A graduate-level google-proof q&a benchmark. In *First Conference on Language Modeling*, 2024.

[Sui *et al.*, 2025] Yang Sui, Yu-Neng Chuang, Guanchu Wang, Jiamu Zhang, Tianyi Zhang, Jiayi Yuan, Hongyi Liu, Andrew Wen, Shaochen Zhong, Na Zou, et al. Stop overthinking: A survey on efficient reasoning for large language models. *arXiv preprint arXiv:2503.16419*, 2025.

[Team *et al.*, 2025] Kimi Team, Angang Du, Bofei Gao, Bowei Xing, Changjiu Jiang, Cheng Chen, Cheng Li, Chenjun Xiao, Chenzhuang Du, Chonghua Liao, et al. Kimi k1. 5: Scaling reinforcement learning with llms. *arXiv preprint arXiv:2501.12599*, 2025.

[Utans, 1996] Joachim Utans. Weight averaging for neural networks and local resampling schemes. In *Proc. AAAI-96 Workshop on Integrating Multiple Learned Models*. AAAI Press, pages 133–138. Citeseer, 1996.

[Wei *et al.*, 2022] Jason Wei, Xuezhi Wang, Dale Schuurmans, Maarten Bosma, Fei Xia, Ed Chi, Quoc V Le, Denny Zhou, et al. Chain-of-thought prompting elicits reasoning in large language models. *Advances in neural information processing systems*, 35:24824–24837, 2022.

[Williams and Rasmussen, 2006] Christopher KI Williams and Carl Edward Rasmussen. *Gaussian processes for machine learning*, volume 2. MIT press Cambridge, MA, 2006.

[Wu *et al.*, 2025] Taiqiang Wu, Runming Yang, Tao Liu, Jia-hao Wang, and Ngai Wong. Revisiting model interpolation for efficient reasoning. *arXiv preprint arXiv:2510.10977*, 2025.

[Yadav *et al.*, 2023] Prateek Yadav, Derek Tam, Leshem Choshen, Colin A Raffel, and Mohit Bansal. Ties-merging: Resolving interference when merging models. *Advances in Neural Information Processing Systems*, 36:7093–7115, 2023.

[Yang *et al.*, 2024] Enneng Yang, Li Shen, Guibing Guo, Xingwei Wang, Xiaochun Cao, Jie Zhang, and Dacheng Tao. Model merging in llms, mllms, and beyond: Methods, theories, applications and opportunities. *arXiv preprint arXiv:2408.07666*, 2024.

[Yang *et al.*, 2025] An Yang, Anfeng Li, Baosong Yang, Beichen Zhang, Binyuan Hui, Bo Zheng, Bowen Yu, Chang Gao, Chengan Huang, Chenxu Lv, et al. Qwen3 technical report. *arXiv preprint arXiv:2505.09388*, 2025.

[Yu *et al.*, 2024] Le Yu, Bowen Yu, Haiyang Yu, Fei Huang, and Yongbin Li. Language models are super mario: Absorbing abilities from homologous models as a free lunch. In *Forty-first International Conference on Machine Learning*, 2024.

## A Analysis and Implementation of Block Partitioning

This appendix consolidates (i) the analysis of layer-wise task-vector differences and (ii) the formal implementation of the block partitioning strategy used for the granularity comparison in our experiments.

### A.1 Layer-wise Difference Analysis and Visualization

Figure 8 visualizes the layer-wise  $\ell_1$ -norm and  $\ell_2$ -norm differences between the base model and expert models. We observe that the parameter differences are primarily concentrated in deeper layers, while shallow layers remain relatively stable. This aligns with the common understanding that deeper layers contribute more to high-level semantic processing (e.g., logical reasoning), whereas earlier layers capture more general, transferable features.

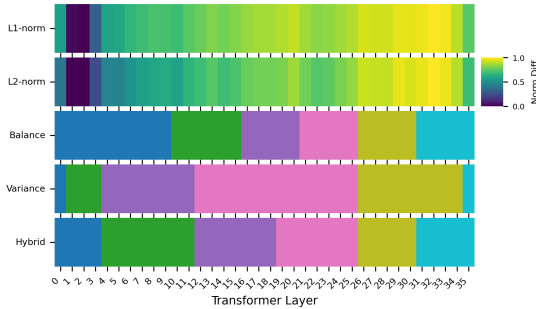


Figure 8: Visualization of layer-wise  $\ell_1/\ell_2$  differences between task models and the resulting block partition strategies (Balance-only, Variance-only, and Hybrid).

### A.2 Partitioning Strategies

Because layer-wise differences are non-uniform across depth, we compare three partitioning strategies:

- **Balance-only.** Enforces equal total difference per block. This often yields highly uneven block sizes (e.g., a single active deep layer forms a block, while many stable shallow layers are grouped together), which can distort the effective granularity of decision variables.
- **Variance-only.** Groups layers with similar difference magnitudes (e.g., Fisher–Jenks natural breaks), improving within-block homogeneity. However, it may result in blocks carrying very different amounts of “information mass”, creating imbalance across decision variables.
- **Hybrid strategy (ours).** Optimizes a trade-off between within-block homogeneity and across-block balance, typically isolating highly active deep layers into smaller, homogeneous blocks while keeping a reasonable distribution of total difference across blocks.

### A.3 Formal Formulation and Dynamic Programming Algorithm

We cast layer partitioning as a variant of Fisher–Jenks natural breaks. Let  $\{d_l\}_{l=1}^L$  denote a non-negative per-layer difference score computed from task vectors. We aim to partition

#### Algorithm 2 Hybrid Optimal Block Partitioning

---

```

1: Input: Task vectors  $\{TV_l^{(i)}\}$  for layers  $l = 1, \dots, L$ , number of blocks  $K$ , balance weight  $\lambda$ 
2: Output: Block partition  $\mathcal{P} = \{B_1, \dots, B_K\}$ 
3: Compute per-layer scores:
   
$$d_l \leftarrow \sum_{i=1}^N \left\| TV_l^{(i)} - \text{mean}(TV_l^{(i)}) \right\|_p$$

4: Target  $\leftarrow \left( \sum_{l=1}^L d_l \right) / K$ 
5: Precompute block costs for all  $1 \leq i \leq j \leq L$ :
   
$$\mathcal{C}(i, j) \leftarrow \text{Var}(d_{i:j}) \cdot (j - i + 1) + \lambda \cdot (\text{Sum}(d_{i:j}) - \text{Target})^2$$

6: Initialize  $\text{DP}[k][l] \leftarrow +\infty$ ; set  $\text{DP}[0][0] \leftarrow 0$ 
7: for  $k = 1$  to  $K$  do
8:   for  $l = 1$  to  $L$  do
9:     for  $m = k - 1$  to  $l - 1$  do
10:      if  $\text{DP}[k-1][m] + \mathcal{C}(m+1, l) < \text{DP}[k][l]$  then
11:         $\text{DP}[k][l] \leftarrow \text{DP}[k-1][m] + \mathcal{C}(m+1, l)$ 
12:         $\text{Split}[k][l] \leftarrow m$ 
13:      end if
14:    end for
15:  end for
16: end for
17: Reconstruct  $\mathcal{P}$  by backtracking  $\text{Split}[K][L]$ .

```

---

$L$  layers into  $K$  contiguous blocks  $\mathcal{P} = \{B_1, \dots, B_K\}$  that minimize a hybrid objective:

$$\min_{\mathcal{P}} J(\mathcal{P}) = \sum_{k=1}^K \text{Cost}(B_k) = \sum_{k=1}^K (\text{Var}(B_k) + \lambda \cdot \text{Dev}(B_k)), \quad (9)$$

where  $\text{Var}(B_k)$  is the within-block variance and  $\text{Dev}(B_k)$  penalizes deviation from a target block sum:

$$\text{Var}(B_k) = \sum_{l \in B_k} (d_l - \mu_{B_k})^2, \quad (10)$$

$$\text{Dev}(B_k) = \left( \sum_{l \in B_k} d_l - \text{Target} \right)^2, \quad (11)$$

$$\text{Target} = \frac{\sum_{l=1}^L d_l}{K}. \quad (12)$$

Here,  $\mu_{B_k}$  denotes the mean of  $\{d_l : l \in B_k\}$ , and  $\lambda \geq 0$  controls the balance–homogeneity trade-off.

We solve this optimization via dynamic programming (DP). Define  $\mathcal{C}(i, j)$  as the cost of forming a block containing contiguous layers  $i, \dots, j$ . Then:

$$\text{DP}[k][l] = \min_{m \in \{k-1, \dots, l-1\}} \{\text{DP}[k-1][m] + \mathcal{C}(m+1, l)\}, \quad (13)$$

with  $\text{DP}[0][0] = 0$  and  $\text{DP}[0][l > 0] = +\infty$ . The optimal partition is recovered by backtracking the split points.

#### A.4 Proof of Optimality

**Theorem 1.** Let  $\text{DP}[k][l]$  be defined by the recurrence

$$\text{DP}[k][l] = \min_m \{\text{DP}[k-1][m] + \mathcal{C}(m+1, l)\},$$

with standard base cases. Then  $\text{DP}[K][L]$  equals the globally minimum cost for partitioning  $L$  layers into  $K$  contiguous blocks under the additive objective  $\sum_{k=1}^K \text{Cost}(B_k)$ .

*Proof.* We prove by induction on  $k$ . For  $k = 1$ , there is only one feasible partition: a single block covering all layers  $1:l$ , and the DP value matches this cost. Assume for  $k - 1$  that  $\text{DP}[k-1][m]$  equals the minimum cost among all partitions of the first  $m$  layers into  $k - 1$  blocks. For  $k$  blocks partitioning the first  $l$  layers, any feasible solution must end with some final block  $(m+1):l$ , preceded by a valid partition of  $1:m$  into  $k - 1$  blocks. By the inductive hypothesis, the minimum achievable cost of the prefix is  $\text{DP}[k-1][m]$ , hence the total cost is at least  $\text{DP}[k-1][m] + \mathcal{C}(m+1, l)$ . Taking the minimum over all valid split points  $m$  yields exactly the global optimum, which is the DP recurrence. Therefore,  $\text{DP}[K][L]$  is globally optimal.  $\square$

## B Detailed Baseline Formulations

This appendix provides the mathematical definitions for model-level merging baselines used in our experiments. Let  $\mathcal{M}^{(\text{base})}$  be the base model and  $\mathcal{M}^{(i)}$  the  $i$ -th expert model. Define the task vector

$$TV^{(i)} := \mathcal{M}^{(i)} - \mathcal{M}^{(\text{base})}.$$

### B.1 Task Arithmetic

Task Arithmetic steers the base model by adding a weighted sum of task vectors:

$$\mathcal{M}^{(\text{merge})} = \mathcal{M}^{(\text{base})} + \alpha \sum_{i=1}^T TV^{(i)}. \quad (14)$$

### B.2 TIES-Merging

TIES addresses parameter conflicts using sparsification, sign resolution, and selective merging. A simplified form can be written as:

$$\mathcal{M}^{(\text{merge})} = \mathcal{M}^{(0)} + \alpha \cdot \text{top-k}\left(TV^{(i)}\right), \quad (15)$$

where  $\text{top-k}(\cdot)$  keeps the largest-magnitude parameters.

### B.3 DARE-Merging

DARE (Drop And REscale) randomly drops a fraction  $p$  of delta parameters and rescales the rest:

$$\mathcal{M}^{(\text{merge})} = \mathcal{M}^{(\text{base})} + \alpha \sum_{i=1}^T \text{DARE}\left(TV^{(i)}, p\right). \quad (16)$$

### B.4 Breadcrumbs

Breadcrumbs applies sparsification and masking to remove both large outliers and small perturbations:

$$\mathcal{M}^{(\text{merge})} = \mathcal{M}^{(\text{base})} + \alpha \sum_{i=1}^T m^{(i)} \odot TV^{(i)}, \quad (17)$$

where  $m^{(i)}$  is a mask and  $\odot$  denotes element-wise multiplication.

## B.5 DELLA

DELLA (Drop–Elect–Fuse) drops parameters, elects deltas with consistent signs, and fuses them:

$$\mathcal{M}^{(\text{merge})} = \mathcal{M}^{(\text{base})} + \lambda \cdot \delta^{(\text{avg})}, \quad (18)$$

where  $\delta^{(\text{avg})}$  is the averaged and rescaled delta after the Drop–Elect–Fuse pipeline.

## C Detailed Experimental Results

Table 8 reports the complete set of evaluated configurations across different merging granularities.

## D Surrogate Model and Kernel Specifications

### D.1 ARD Matérn-5/2 Kernel

To model the non-linear landscape of LLM merging, we use the Matérn-5/2 kernel with Automatic Relevance Determination (ARD). For two configurations  $\mathbf{x}, \mathbf{x}' \in [0, 1]^D$ , the kernel is:

$$k(\mathbf{x}, \mathbf{x}') = \sigma_f^2 \left( 1 + \sqrt{5}r + \frac{5}{3}r^2 \right) \exp(-\sqrt{5}r), \quad (19)$$

where

$$r(\mathbf{x}, \mathbf{x}') = \sqrt{\sum_{d=1}^D \frac{(x_d - x'_d)^2}{\ell_d^2}}. \quad (20)$$

### D.2 Hierarchical SAAS Prior for Sparsity

In high-dimensional LLM merging, most layers may have negligible impact on the resulting Pareto frontier. Following [Eriksson and Jankowiak, 2021], we place a Sparse Axis-Aligned Subspace (SAAS) prior on the inverse squared lengthscales  $\rho_d = 1/\ell_d^2$ :

$$\tau \sim \text{Half-Cauchy}(0.1), \quad \rho_d \sim \text{Half-Cauchy}(\tau), \quad d = 1, \dots, D. \quad (21)$$

Here  $\tau$  is a global shrinkage parameter encouraging most  $\rho_d$  to be near zero (i.e.,  $\ell_d \rightarrow \infty$ ), effectively pruning irrelevant dimensions; only a few critical dimensions with large  $\rho_d$  remain active.

### D.3 Fully Bayesian Inference via NUTS

Unlike standard Bayesian optimization that often uses MLE/MAP for hyperparameter fitting, SIP-BMM uses fully Bayesian inference to account for hyperparameter uncertainty, which is particularly important when the evaluation budget is small. Let  $\theta = \{\rho_{1:D}, \sigma_f^2, \sigma_e^2\}$  denote GP hyperparameters. We infer:

$$p(\theta | \mathcal{D}) \propto p(\mathcal{Y} | \mathcal{X}, \theta) p(\theta), \quad (22)$$

and draw samples  $\{\theta^{(m)}\}_{m=1}^M$  using the No-U-Turn Sampler (NUTS). The acquisition function is integrated over hyperparameter samples:

$$\alpha(\mathbf{x}) = \frac{1}{M} \sum_{m=1}^M \alpha(\mathbf{x}; \theta^{(m)}). \quad (23)$$

## D.4 SIP-Guided Warm-Start for NUTS Initialization

The efficiency of NUTS in high dimensions depends on chain initialization. We use the Structural Importance Prior (SIP) to warm-start the initial lengthscales by setting  $\ell_d$  to SIP-derived values  $\ell_d^{(0)}$  (as defined in the main paper). Since the kernel sensitivity to dimension  $d$  scales as  $|\partial k / \partial x_d| \propto 1/\ell_d^2$ , initializing critical layers with smaller  $\ell_d^{(0)}$  (e.g., 0.5) biases early sampling toward functionally active dimensions, while stable layers can be initialized with larger values (e.g., 5.0). This enables SIP-BMM to approach the Pareto frontier more quickly than vanilla SAASBO under limited evaluations.

## E qNEHVI Implementation Details

**Attribution.** We use the  $q$ NEHVI acquisition and the corresponding log-stabilized Monte-Carlo estimator from [Daulton *et al.*, 2022].

**Decision space and objective vector (same as main text).** Our decision variable is the layer-wise merging vector  $\mathbf{x} \in [0, 1]^D$  with  $D = L$ ,

$$\mathbf{x} = (x_1, \dots, x_L), \quad x_l \in [0, 1], \quad l = 1, \dots, L. \quad (24)$$

Each  $\mathbf{x}$  defines a merged model  $\mathcal{M}_{\text{merge}}(\mathbf{x}) = \text{Layer-Wise-Merge}(\{\mathcal{M}_i\}; \mathbf{x})$ , which is evaluated by the  $K$  normalized objectives  $y_k(\mathbf{x}) := f_k(\mathcal{M}_{\text{merge}}(\mathbf{x}))$ . We collect them into the objective vector

$$\mathbf{y}(\mathbf{x}) = (y_1(\mathbf{x}), \dots, y_K(\mathbf{x})) = (f_1(\mathcal{M}_{\text{merge}}(\mathbf{x})), \dots, f_K(\mathcal{M}_{\text{merge}}(\mathbf{x}))) \in \mathbb{R}^K. \quad (25)$$

All objectives are maximized in this normalized space.

**Data at iteration  $t$  and observed nondominated set.** At BO iteration  $t$ , we have the evaluation dataset  $\mathcal{D}_t = \{(\mathbf{x}_i, \mathbf{y}_i)\}_{i=1}^{n_t}$  with  $\mathbf{y}_i = \mathbf{y}(\mathbf{x}_i)$ . Let

$$\mathcal{P}_t \subseteq \{\mathbf{y}_i\}_{i=1}^{n_t} \quad (26)$$

denote the set of *observed* nondominated objective vectors (Pareto set in objective space). Let  $\mathbf{r} \in \mathbb{R}^K$  be a fixed reference point.

**Hypervolume improvement (HVI).** Given  $q$  new objective vectors  $\mathbf{Y} = \{\mathbf{y}^{(1)}, \dots, \mathbf{y}^{(q)}\}$ , the deterministic hypervolume improvement is

$$\text{HVI}(\mathbf{Y}; \mathcal{P}_t, \mathbf{r}) = \text{HV}(\mathcal{P}_t \cup \mathbf{Y}; \mathbf{r}) - \text{HV}(\mathcal{P}_t; \mathbf{r}), \quad (27)$$

where  $\text{HV}(\cdot; \mathbf{r})$  is the dominated hypervolume w.r.t.  $\mathbf{r}$ .

**Noisy Pareto samples  $\tilde{\mathcal{P}}_t$  (accounting for observation noise).** We fit a multi-objective surrogate at iteration  $t$  as  $K$  independent SAAS GPs to model each scalar objective  $y_k(\mathbf{x})$ . In the noisy EHVI setting, the nondominated set used in HVI is treated as random:  $\tilde{\mathcal{P}}_t$  is formed by sampling latent (noise-free) outcomes of the already-evaluated points from the GP posterior and taking the nondominated subset [Daulton *et al.*, 2022]. Concretely, for each Monte-Carlo draw  $n = 1, \dots, N$  we sample

$$\tilde{\mathbf{y}}_i^{(n)} \sim p(\mathbf{y}(\mathbf{x}_i) \mid \mathcal{D}_t), \quad i = 1, \dots, n_t, \quad (28)$$

and define

$$\tilde{\mathcal{P}}_t^{(n)} := \text{ND}\left(\{\tilde{\mathbf{y}}_i^{(n)}\}_{i=1}^{n_t}\right), \quad (29)$$

where  $\text{ND}(\cdot)$  returns the nondominated subset under Pareto dominance (maximization).

**$q$ NEHVI acquisition for a batch of merge vectors.** We optimize a batch of  $q$  candidate merge vectors  $\mathbf{X} = \{\mathbf{x}^{(i)}\}_{i=1}^q \subset [0, 1]^D$ . This batch induces random objective vectors under the GP posterior:

$$\mathbf{Y}(\mathbf{X}) = \{\mathbf{y}(\mathbf{x}^{(i)})\}_{i=1}^q. \quad (30)$$

The  $q$ NEHVI acquisition is the posterior expectation

$$\alpha_{q\text{NEHVI}}(\mathbf{X}) = \mathbb{E}_{\tilde{\mathcal{P}}_t, \mathbf{Y}(\mathbf{X}) \mid \mathcal{D}_t} [\text{HVI}(\mathbf{Y}(\mathbf{X}); \tilde{\mathcal{P}}_t, \mathbf{r})], \quad (31)$$

**Monte-Carlo estimator and log-stabilized evaluation.** We approximate Eq. (31) with Monte-Carlo samples from the *joint* posterior of the batch outcomes:

$$\hat{\alpha}_{q\text{NEHVI}}^{(N)}(\mathbf{X}) = \frac{1}{N} \sum_{n=1}^N \text{HVI}\left(\mathbf{Y}^{(n)}(\mathbf{X}); \tilde{\mathcal{P}}_t^{(n)}, \mathbf{r}\right), \quad (32)$$

where  $\mathbf{Y}^{(n)}(\mathbf{X})$  is the  $n$ -th posterior draw of  $\mathbf{Y}(\mathbf{X})$  and  $\tilde{\mathcal{P}}_t^{(n)}$  is the corresponding noisy Pareto sample defined above. Following [Daulton *et al.*, 2022], we compute the MC objective using a log-stabilized formulation of the improvement term to avoid numerical underflow/overflow when improvements become very small (common near convergence), while the underlying utility remains (noisy) expected hypervolume improvement.

Table 6: Detailed individual metrics for different merging granularities (full data).

ID	Method	f1 (↑)	f2 (↑)	GPQA_ACC (↑)	GPQA_TOKENS (↓)	AIME25_ACC (↑)	AIME25_TOKENS (↓)	Pareto
0	Layer-wise	0.8698	0.8047	0.6212	4037	0.7666	8891	✓
1		0.9527	0.2414	0.6616	9136	0.7666	15496	✗
2		0.3656	1.0585	0.4545	791	0.6666	7321	✓
3		0.6848	0.8697	0.6364	3427	0.6333	8161	✓
4		0.3428	1.0599	0.4697	958	0.6333	7037	✓
5		0.1783	1.0666	0.4949	764	0.5000	7158	✓
6		0.2116	1.0600	0.4848	717	0.5333	7392	✓
7		0.8826	0.7393	0.6010	4308	0.8000	10132	✓
8		0.5753	1.0409	0.5303	900	0.7000	7602	✓
9		0.6101	0.9011	0.6263	2509	0.6000	8732	✓
0	Block-wise (n=18)	1.0691	0.5632	0.6919	6660	0.8000	11077	✓
1		0.6894	0.7855	0.5859	4706	0.7000	8384	✗
2		0.5086	1.0210	0.5505	1573	0.6333	7106	✗
3		0.7308	0.7012	0.6061	5104	0.7000	9912	✗
4		0.1266	1.0383	0.4697	981	0.5000	7545	✗
5		0.5455	0.9135	0.6212	2698	0.5666	8140	✗
6		0.8677	0.6257	0.6465	6076	0.7333	10369	✗
7		0.7183	0.7383	0.6263	3923	0.6667	10729	✗
8		0.8552	0.6671	0.6667	5376	0.7000	10366	✗
0	Block-wise (n=9)	0.9320	0.4935	0.6515	7576	0.7666	11472	✗
1		0.9735	0.3001	0.6717	8549	0.7666	14888	✗
2		0.8552	0.5161	0.6667	7219	0.7000	11430	✗
3		0.7411	0.6215	0.6111	6391	0.7000	10008	✗
4		0.5628	0.8946	0.5505	1273	0.6667	10726	✗
5		0.6284	0.8021	0.6616	4832	0.5666	7779	✗
6		0.4776	0.9933	0.5354	1680	0.6333	7643	✗
7		1.0611	0.2645	0.6616	8242	0.8334	16240	✗
8		0.7930	0.6184	0.6364	6471	0.7000	9968	✗
9	Model-level	1.0818	0.2037	0.6717	8082	0.8334	18005	✗
10		0.3822	1.0249	0.5152	1226	0.6000	7520	✗
11		1.0715	0.2445	0.6667	8176	0.8334	16841	✗
12		1.0506	0.2790	0.6566	8406	0.8333	15631	✗
13		0.9506	0.3431	0.6869	8263	0.7333	14233	✗
0		0.4983	0.9734	0.5455	1441	0.6333	8496	✗
1		0.5168	0.9129	0.5808	3197	0.6000	7417	✗
2		0.5227	0.7743	0.6364	4966	0.5333	8279	✗
3		0.6516	0.6855	0.6465	6165	0.6000	8735	✗
4		0.5812	0.7023	0.5859	6368	0.6333	8013	✗
5		0.7700	0.6019	0.6515	7065	0.6667	9503	✗
6		0.8012	0.5726	0.6667	7220	0.6667	10008	✗
7		0.8885	0.5154	0.6566	7697	0.7333	10740	✗
8		0.8906	0.3548	0.6313	8851	0.7666	13067	✗
9	AIME25	1.0691	0.3285	0.6919	8812	0.8000	13786	✗
10		1.0923	0.3010	0.6768	8571	0.8334	14834	✓
11		1.1231	0.2153	0.6919	8443	0.8333	17178	✓
12		1.1438	0.2042	0.7020	8560	0.8333	17285	✓

## Evaluation Results for Selected LLM Pareto Solutions

Table 7: Evaluation Results for Selected LLM Pareto Solutions

Solution ID	Content
1	<p><b>Question:</b> Answer the following multiple choice question. The last line of your response should be of the following format: 'ANSWER: \$LETTER' (without quotes) where LETTER is one of A,B,C,D. Think step by step before answering.</p> <p>Two quantum states with energies <math>E_1</math> and <math>E_2</math> have a lifetime of <math>10^{-9}</math> sec and <math>10^{-8}</math> sec, respectively. We want to clearly distinguish these two energy levels. Which one of the following options could be their energy difference so that they can be clearly resolved?</p> <p><b>Options:</b> A) <math>10^{-9}</math> eV B) <math>10^{-8}</math> eV C) <math>10^{-4}</math> eV D) <math>10^{-11}</math> eV</p> <p><b>Model Answer:</b> C <b>Correct Answer:</b> C <b>Character Count:</b> 454.0</p> <p><b>Full Answer:</b> To determine the energy difference that allows clear resolution between two quantum states, we need to consider the energy uncertainty principle, which relates the energy of a state to its lifetime. The energy-time uncertainty principle states that: <math>\Delta E \cdot \Delta t \geq \frac{\hbar}{2}</math> where: - <math>\Delta E</math> is the energy uncertainty (related to the energy difference we want to resolve) - <math>\Delta t</math> is the lifetime of the state - <math>\hbar</math> is the reduced Planck's constant (<math>\approx 6.582 \times 10^{-16}</math> eV·s)</p> <p>For a state with lifetime <math>\Delta t</math>, the energy uncertainty is approximately: <math>\Delta E \approx \hbar/\Delta t</math></p> <p>So for each state: For <math>E_1</math> with <math>\Delta t = 10^{-9}</math> sec: <math>\Delta E_1 \approx (6.582 \times 10^{-16} \text{ eV}\cdot\text{s}) / (10^{-9} \text{ s}) = 6.582 \times 10^{-7} \text{ eV} \approx 10^{-6} \text{ eV}</math></p> <p>For <math>E_2</math> with <math>\Delta t = 10^{-8}</math> sec: <math>\Delta E_2 \approx (6.582 \times 10^{-16} \text{ eV}\cdot\text{s}) / (10^{-8} \text{ s}) = 6.582 \times 10^{-8} \text{ eV} \approx 10^{-7} \text{ eV}</math></p> <p>The energy difference between the two states must be larger than the energy uncertainty of each state to be resolved. So we need an energy difference larger than both <math>\Delta E_1</math> and <math>\Delta E_2</math>.</p> <p>Looking at the options: A) <math>10^{-9}</math> eV (too small) B) <math>10^{-8}</math> eV (smaller than <math>\Delta E_2</math>) C) <math>10^{-4}</math> eV (larger than both <math>\Delta E_1</math> and <math>\Delta E_2</math>) D) <math>10^{-11}</math> eV (too small)</p> <p>Option C (<math>10^{-4}</math> eV) is the only one that is larger than both energy uncertainties and thus can be clearly resolved.</p> <p>ANSWER: C</p>
2	<p><b>Question:</b> Answer the following multiple choice question. The last line of your response should be of the following format: 'ANSWER: \$LETTER' (without quotes) where LETTER is one of A,B,C,D. Think step by step before answering.</p> <p>Two quantum states with energies <math>E_1</math> and <math>E_2</math> have a lifetime of <math>10^{-9}</math> sec and <math>10^{-8}</math> sec, respectively. We want to clearly distinguish these two energy levels. Which one of the following options could be their energy difference so that they can be clearly resolved?</p> <p><b>Options:</b> A) <math>10^{-9}</math> eV B) <math>10^{-8}</math> eV C) <math>10^{-4}</math> eV D) <math>10^{-11}</math> eV</p> <p><b>Model Answer:</b> C <b>Correct Answer:</b> C <b>Character Count:</b> 457.0</p> <p><b>Full Answer:</b> To determine which energy difference allows us to clearly distinguish the two quantum states, we need to consider the uncertainty principle, specifically the energy-time uncertainty relation: <math>\Delta E \cdot \Delta t \geq \frac{\hbar}{2}</math> Where: - <math>\Delta E</math> is the energy uncertainty - <math>\Delta t</math> is the lifetime of the state - <math>\hbar</math> is the reduced Planck constant (<math>\approx 6.58 \times 10^{-16}</math> eV·s)</p> <p>For a state with lifetime <math>\Delta t</math>, the energy uncertainty <math>\Delta E</math> is approximately <math>\hbar/\Delta t</math>.</p> <p>Let's calculate the energy uncertainty for each lifetime:</p> <p>For <math>\Delta t = 10^{-9}</math> sec: <math>\Delta E \approx \frac{6.58 \times 10^{-16} \text{ eV}\cdot\text{s}}{10^{-9} \text{ s}} = 6.58 \times 10^{-7} \text{ eV}</math></p> <p>For <math>\Delta t = 10^{-8}</math> sec: <math>\Delta E \approx \frac{6.58 \times 10^{-16} \text{ eV}\cdot\text{s}}{10^{-8} \text{ s}} = 6.58 \times 10^{-8} \text{ eV}</math></p> <p>The energy difference between the two states must be larger than the energy uncertainty of the shorter-lived state (since it has the larger uncertainty) to be clearly resolved. The shorter-lived state has a larger energy uncertainty (<math>10^{-9}</math> sec has larger uncertainty than <math>10^{-8}</math> sec).</p> <p>So the energy difference should be larger than the larger of these two uncertainties (<math>6.58 \times 10^{-8} \text{ eV} \approx 10^{-7} \text{ eV}</math>).</p> <p>Looking at the options: A) <math>10^{-9}</math> eV (too small) B) <math>10^{-8}</math> eV (smaller than <math>10^{-7}</math> eV, so not clearly resolved) C) <math>10^{-4}</math> eV (larger than <math>10^{-7}</math> eV, so it could be resolved) D) <math>10^{-11}</math> eV (too small)</p> <p>Option C (<math>10^{-4}</math> eV) is the only one that is larger than the energy uncertainty of the shorter-lived state (<math>10^{-7}</math> eV), so it would allow clear distinction.</p> <p>ANSWER: C</p>

*Continued on next page*

Table 7 – *Continued from previous page*

ID	Content
3	<p><b>Question:</b> Answer the following multiple choice question. The last line of your response should be of the following format: 'ANSWER: \$LETTER' (without quotes) where LETTER is one of A,B,C,D. Think step by step before answering.</p> <p>Two quantum states with energies <math>E_1</math> and <math>E_2</math> have a lifetime of <math>10^{-9}</math> sec and <math>10^{-8}</math> sec, respectively. We want to clearly distinguish these two energy levels. Which one of the following options could be their energy difference so that they can be clearly resolved?</p> <p><b>Options:</b> A) <math>10^{-9}</math> eV B) <math>10^{-8}</math> eV C) <math>10^{-4}</math> eV D) <math>10^{-11}</math> eV</p> <p><b>Model Answer:</b> C <b>Correct Answer:</b> C <b>Character Count:</b> 459.0</p> <p><b>Full Answer:</b> To determine which energy difference would allow us to clearly distinguish the two energy levels, I need to consider the uncertainty principle. The energy-time uncertainty principle states that <math>\Delta E \cdot \Delta t \geq \hbar/2</math>, where <math>\Delta E</math> is the energy uncertainty and <math>\Delta t</math> is the lifetime of the state.</p> <p>For each state: - State 1 has a lifetime of <math>10^{-9}</math> sec, so <math>\Delta E_1 \approx \hbar/(2 \times 10^{-9})</math> - State 2 has a lifetime of <math>10^{-8}</math> sec, so <math>\Delta E_2 \approx \hbar/(2 \times 10^{-8})</math></p> <p>The energy difference <math>\Delta E</math> between the two states must be larger than the individual energy uncertainties to be clearly resolved. So we need <math>\Delta E &gt; \max(\Delta E_1, \Delta E_2)</math>.</p> <p>Let's calculate the energy uncertainties approximately: - <math>\hbar \approx 6.582 \times 10^{-16}</math> eV·s - <math>\Delta E_1 \approx 6.582 \times 10^{-16}/(2 \times 10^{-9}) \approx 3.29 \times 10^{-7}</math> eV - <math>\Delta E_2 \approx 6.582 \times 10^{-16}/(2 \times 10^{-8}) \approx 3.29 \times 10^{-8}</math> eV</p> <p>So the larger uncertainty is <math>\Delta E_1 \approx 3.29 \times 10^{-7}</math> eV. Therefore, the energy difference must be larger than this value to be clearly resolved.</p> <p>Looking at the options: A) <math>10^{-9}</math> eV - too small B) <math>10^{-8}</math> eV - still smaller than <math>3.29 \times 10^{-7}</math> eV C) <math>10^{-4}</math> eV - larger than <math>3.29 \times 10^{-7}</math> eV D) <math>10^{-11}</math> eV - too small</p> <p>Option C is the only one that is larger than the larger energy uncertainty (<math>3.29 \times 10^{-7}</math> eV), so it would allow clear resolution of the two energy levels.</p> <p>ANSWER: C</p>
4	<p><b>Question:</b> Answer the following multiple choice question. The last line of your response should be of the following format: 'ANSWER: \$LETTER' (without quotes) where LETTER is one of A,B,C,D. Think step by step before answering.</p> <p>Two quantum states with energies <math>E_1</math> and <math>E_2</math> have a lifetime of <math>10^{-9}</math> sec and <math>10^{-8}</math> sec, respectively. We want to clearly distinguish these two energy levels. Which one of the following options could be their energy difference so that they can be clearly resolved?</p> <p><b>Options:</b> A) <math>10^{-9}</math> eV B) <math>10^{-8}</math> eV C) <math>10^{-4}</math> eV D) <math>10^{-11}</math> eV</p> <p><b>Model Answer:</b> C <b>Correct Answer:</b> C <b>Character Count:</b> 2983.0</p> <p><b>Full Answer:</b> First, I need to recall the relationship between the lifetime of a quantum state and the energy uncertainty. This comes from the Heisenberg uncertainty principle, which states that the product of the uncertainty in energy (<math>\Delta E</math>) and the uncertainty in time (<math>\Delta t</math>) is approximately <math>\hbar/2</math>. For a state with a lifetime <math>\tau</math>, the energy uncertainty is roughly <math>\Delta E \approx \hbar/\tau</math>.</p> <p>The uncertainty principle is <math>\Delta E \cdot \Delta t \geq \hbar/2</math>. For a state with lifetime <math>\tau</math>, we often take <math>\Delta t \approx \tau</math>, so <math>\Delta E \approx \hbar/(2\tau)</math>. But for rough estimates, we can say <math>\Delta E \approx \hbar/\tau</math>.</p> <p>Now, <math>\hbar</math> is the reduced Planck's constant. I remember that <math>\hbar = h/(2\pi)</math>, and <math>h</math> is about <math>4.135667662 \times 10^{-15}</math> eV·s (I think it's better to use a standard value). I know that <math>\hbar c</math> is often used in particle physics, but for energy, let's think in eV and seconds.</p> <p>A common approximation is that <math>\hbar \approx 6.582 \times 10^{-16}</math> eV·s. Let me confirm that.</p> <p>Yes, <math>\hbar = h/(2\pi) \approx (4.135667662 \times 10^{-15})/(2\pi) \approx 6.582 \times 10^{-16}</math> eV·s. That sounds right.</p> <p>So, <math>\Delta E \approx \hbar/\tau</math>.</p> <p>Now, the problem gives lifetimes: <math>\tau_1 = 10^{-9}</math> sec for <math>E_1</math>, <math>\tau_2 = 10^{-8}</math> sec for <math>E_2</math>.</p> <p>We want to clearly distinguish these two energy levels. That means the energy difference between them should be larger than the energy uncertainty of each state.</p> <p>To resolve two energy levels, the energy difference <math>\Delta E</math> should be greater than the larger of the two energy uncertainties, because if it's smaller than both, they might not be distinguishable.</p> <p>The uncertainty for <math>E_1</math> is <math>\Delta E_1 \approx \hbar/\tau_1</math>, and for <math>E_2</math> is <math>\Delta E_2 \approx \hbar/\tau_2</math>.</p> <p>Since <math>\tau_1 = 10^{-9}</math> s and <math>\tau_2 = 10^{-8}</math> s, <math>\tau_1</math> is smaller than <math>\tau_2</math>, so <math>\Delta E_1</math> should be larger than <math>\Delta E_2</math> because <math>\Delta E</math> is inversely proportional to <math>\tau</math>.</p>

*Continued on next page*

Table 7 – *Continued from previous page*

ID	Content
4	<p>Let me calculate the uncertainties.</p> <p>First, for <math>E_1</math>: <math>\tau_1 = 1.0 \times 10^{-9}</math> s  <math>\Delta E_1 \approx \hbar/\tau_1 \approx (6.582 \times 10^{-16} \text{ eV}\cdot\text{s})/(1.0 \times 10^{-9} \text{ s}) = 6.582 \times 10^{-7} \text{ eV}</math></p> <p>Similarly, for <math>E_2</math>: <math>\tau_2 = 1.0 \times 10^{-8}</math> s  <math>\Delta E_2 \approx \hbar/\tau_2 \approx (6.582 \times 10^{-16} \text{ eV}\cdot\text{s})/(1.0 \times 10^{-8} \text{ s}) = 6.582 \times 10^{-8} \text{ eV}</math></p> <p>So, <math>\Delta E_1 \approx 6.6 \times 10^{-7} \text{ eV}</math> and <math>\Delta E_2 \approx 6.6 \times 10^{-8} \text{ eV}</math>.</p> <p>The larger uncertainty is <math>\Delta E_1 \approx 10^{-6.18} \text{ eV}</math>, which is about <math>6.6 \times 10^{-7} \text{ eV}</math>, so roughly <math>10^{-6} \text{ eV}</math>.</p> <p>To clearly distinguish the two energy levels, the energy difference <math>\Delta E</math> between them should be larger than the larger uncertainty, which is <math>\Delta E_1 \approx 10^{-6} \text{ eV}</math>.</p> <p>Now, looking at the options:</p> <p>A) <math>10^{-9} \text{ eV}</math>  B) <math>10^{-8} \text{ eV}</math>  C) <math>10^{-4} \text{ eV}</math>  D) <math>10^{-11} \text{ eV}</math> <math>10^{-4} \text{ eV}</math> is 0.0001 eV, which is larger than <math>10^{-6} \text{ eV}</math> (0.000001 eV). <math>10^{-4}</math> is 100 times larger than <math>10^{-6}</math>.</p> <p><math>10^{-9} \text{ eV}</math> is smaller than <math>10^{-6} \text{ eV}</math>, <math>10^{-8}</math> is also smaller, <math>10^{-11}</math> is much smaller.</p> <p>So, only option C, <math>10^{-4} \text{ eV}</math>, is larger than the larger uncertainty <math>\Delta E_1 \approx 10^{-6} \text{ eV}</math>.</p> <p>I should double-check the uncertainty calculation.</p> <p>Sometimes the uncertainty is given as <math>\Delta E = \hbar/(2\tau)</math>, but for comparison purposes, the factor of 2 doesn't change the order of magnitude.</p> <p>Let me calculate numerically.</p> <p><math>\hbar = 1.0545718 \times 10^{-34} \text{ J}\cdot\text{s}</math></p> <p>But we need eV.</p> <p><math>1 \text{ eV} = 1.60217662 \times 10^{-19} \text{ J}</math></p> <p>So <math>\hbar</math> in <math>\text{eV}\cdot\text{s} = (1.0545718 \times 10^{-34})/(1.60217662 \times 10^{-19}) \approx 6.582 \times 10^{-16} \text{ eV}\cdot\text{s}</math>, as I had.</p> <p><math>\tau_1 = 10^{-9} \text{ s}</math>  <math>\Delta E_1 = \hbar/\tau_1 = 6.582 \times 10^{-16}/1 \times 10^{-9} = 6.582 \times 10^{-7} \text{ eV} \approx 6.6 \times 10^{-7} \text{ eV}</math></p> <p>Similarly, <math>\Delta E_2 = 6.582 \times 10^{-16}/1 \times 10^{-8} = 6.582 \times 10^{-8} \text{ eV} \approx 6.6 \times 10^{-8} \text{ eV}</math></p> <p>So the energy difference needs to be greater than about <math>10^{-6} \text{ eV}</math> to be resolved from the uncertainty of the first state.</p> <p>Option C is <math>10^{-4} \text{ eV}</math>, which is 0.0001 eV, while <math>10^{-6}</math> is 0.000001, so <math>10^{-4}</math> is 100 times larger, so yes, it should be resolvable.</p> <p>Option A is <math>10^{-9}</math>, which is 0.000000001, much smaller than <math>10^{-6}</math>.</p> <p>B is <math>10^{-8}</math>, still smaller than <math>10^{-6}</math>.</p> <p>D is <math>10^{-11}</math>, even smaller.</p> <p>So only C is larger than the uncertainty.</p> <p>The question says "clearly distinguish these two energy levels". In spectroscopy, to resolve two lines, the energy difference should be larger than the natural width of the lines.</p> <p>The natural width <math>\Gamma = \hbar/\tau</math> for each state.</p> <p>So for <math>E_1</math>, <math>\Gamma_1 = \hbar/\tau_1</math>, for <math>E_2</math>, <math>\Gamma_2 = \hbar/\tau_2</math>.</p> <p>The minimum energy difference to resolve them is roughly the larger of <math>\Gamma_1</math> and <math>\Gamma_2</math>, since if <math>\Delta E &lt; \Gamma_1</math>, they might overlap.</p> <p>In this case, <math>\Gamma_1 &gt; \Gamma_2</math>, so <math>\Delta E &gt; \Gamma_1 \approx 10^{-6} \text{ eV}</math>.</p> <p>Option C is <math>10^{-4} \text{ eV}</math>, which is larger.</p> <p>I recall that in some contexts, for two states to be resolved, <math>\Delta E</math> should be greater than the average or something, but I think the standard is that it should be larger than the energy uncertainty of the state with the shorter lifetime, since it has the broader line.</p> <p>Yes, because the state with shorter lifetime has larger uncertainty, so it's harder to resolve if the energy difference is small.</p> <p>So, for <math>E_1</math> with <math>\tau = 10^{-9} \text{ s}</math>, <math>\Gamma_1</math> is larger, so <math>\Delta E</math> must be <math>&gt; \Gamma_1</math>.</p> <p><math>\Gamma_1 \approx 6.6 \times 10^{-7} \text{ eV}</math>, so <math>10^{-4} \text{ eV}</math> is 100 times larger, so it should be clear.</p> <p>Let me see the options again. Option C is <math>10^{-4} \text{ eV}</math>.</p> <p>Is there a trick? The lifetimes are given, but the energy difference is what we're to choose.</p> <p>Another way: the energy difference should be much larger than the uncertainties.</p> <p>The question says "could be their energy difference so that they can be clearly resolved".</p> <p>So, among the options, which one is larger than the larger uncertainty.</p> <p>Larger uncertainty is <math>\Gamma_1 \approx 10^{-6} \text{ eV}</math> (since <math>6.6 \times 10^{-7}</math> is about <math>10^{-6.2}</math>, so roughly <math>10^{-6}</math>).</p> <p><math>10^{-4}</math> is 100 times larger, so yes.</p> <p><math>10^{-8}</math> is smaller than <math>10^{-6}</math>, so it wouldn't be resolved.</p> <p>For example, if <math>\Delta E = 10^{-8} \text{ eV}</math>, and <math>\Gamma_1 = 10^{-6} \text{ eV}</math>, then <math>\Delta E &lt; \Gamma_1</math>, so the lines would overlap significantly.</p>

*Continued on next page*

Table 7 – *Continued from previous page*

ID	Content
	<p>Similarly, for <math>\Delta E = 10^{-4}</math> eV, it's much larger, so they can be resolved.      I think C is correct.      But let me see why the other options might be tempting.      Option D is <math>10^{-11}</math> eV, which is tiny.      Option A and B are smaller.      Perhaps someone might think that the energy difference should be related to the difference in lifetimes, but no, the uncertainty principle gives the width.      Another thought: in some contexts, for two states, the resolution might depend on the difference in widths, but I think for basic quantum mechanics, it's the energy uncertainty that matters.      The problem says "clearly distinguish these two energy levels", so it's about the energy separation.      I think C is correct.      But let me check the calculation once more.  <math>\hbar = 6.582 \times 10^{-16}</math> eV·s  <math>\tau_1 = 10^{-9}</math> s  <math>\Delta E_1 = 6.582 \times 10^{-16} / 1 \times 10^{-9} = 6.582 \times 10^{-7}</math> eV  <math>6.582 \times 10^{-7}</math> is <math>0.6582 \times 10^{-6}</math>, so approximately <math>10^{-6}</math> eV.  <math>10^{-4}</math> eV is 100 times larger.      Yes.      If I use the formula without the constant, the order of magnitude.      The uncertainty <math>\Delta E \propto 1/\tau</math>.  <math>\tau_1 = 10^{-9}</math>, so <math>\Delta E_1 \propto 10^9</math>  <math>\tau_2 = 10^{-8}</math>, <math>\Delta E_2 \propto 10^8</math>      So <math>\Delta E_1</math> is about 10 times larger than <math>\Delta E_2</math>.      So larger uncertainty is about <math>10^9</math> times <math>\hbar</math>, but in eV.      Since <math>\hbar</math> is fixed, <math>\Delta E_1</math> is 10 times larger than <math>\Delta E_2</math>.      But in terms of the value, <math>\Delta E_1 \approx 10^{-6}</math> eV.      Options: A <math>10^{-9}</math>, B <math>10^{-8}</math>, C <math>10^{-4}</math>, D <math>10^{-11}</math>  <math>10^{-4}</math> is the only one larger than <math>10^{-6}</math>.  <math>10^{-8}</math> is smaller than <math>10^{-6}</math>, since <math>10^{-8} = 0.00000001</math>, <math>10^{-6} = 0.000001</math>, so <math>10^{-6}</math> is larger.      Yes, <math>10^{-6} &gt; 10^{-8}</math>.      So <math>\Delta E</math> must be <math>&gt; 10^{-6}</math> eV, so only C is greater than that.      Therefore, the answer should be C.      I think that's it.      ANSWER: C</p>
5	<p><b>Question:</b> Answer the following multiple choice question. The last line of your response should be of the following format: 'ANSWER: \$LETTER' (without quotes) where LETTER is one of A,B,C,D. Think step by step before answering.</p> <p>Two quantum states with energies <math>E_1</math> and <math>E_2</math> have a lifetime of <math>10^{-9}</math> sec and <math>10^{-8}</math> sec, respectively. We want to clearly distinguish these two energy levels. Which one of the following options could be their energy difference so that they can be clearly resolved?</p> <p><b>Options:</b> A) <math>10^{-9}</math> eV B) <math>10^{-8}</math> eV C) <math>10^{-4}</math> eV D) <math>10^{-11}</math> eV</p> <p><b>Model Answer:</b> C <b>Correct Answer:</b> C <b>Character Count:</b> 6662.0</p> <p><b>Full Answer:</b> First, the question is about distinguishing two quantum states with different lifetimes. The lifetimes are given: <math>E_1</math> has a lifetime of <math>10^{-9}</math> seconds, and <math>E_2</math> has a lifetime of <math>10^{-8}</math> seconds. I need to find which energy difference would allow us to clearly resolve these two levels.</p> <p>I recall that in quantum mechanics, the energy uncertainty is related to the lifetime of the state via the Heisenberg uncertainty principle. The uncertainty in energy, <math>\Delta E</math>, is approximately related to the lifetime <math>\tau</math> by <math>\Delta E \cdot \tau \approx \hbar</math>, where <math>\hbar</math> is the reduced Planck's constant.</p> <p>The Heisenberg uncertainty principle for energy and time is often written as <math>\Delta E \cdot \Delta t \geq \hbar/2</math>, but for practical purposes in spectroscopy, we use <math>\Delta E \approx \hbar/\tau</math>, where <math>\tau</math> is the lifetime.</p>

*Continued on next page*

Table 7 – *Continued from previous page*

ID	Content
5	<p>So, for each state, we can find the energy width due to the finite lifetime. For state <math>E_1</math>, lifetime <math>\tau_1 = 10^{-9}</math> s, so <math>\Delta E_1 \approx \hbar/\tau_1</math>. Similarly, for state <math>E_2</math>, <math>\tau_2 = 10^{-8}</math> s, so <math>\Delta E_2 \approx \hbar/\tau_2</math>. Now, the energy difference between the two states, let's call it <math>\Delta E = E_1 - E_2</math> (in magnitude), needs to be larger than the sum of the energy widths to be resolved. That is, for two peaks to be distinguishable, the energy difference should be greater than the full width at half maximum (FWHM) or something similar. In spectroscopy, if the energy difference is much larger than the individual linewidths, they can be resolved. The linewidth <math>\Gamma</math> for a state is <math>\Gamma = \hbar/\tau</math>, so the uncertainty in energy is <math>\Gamma</math>. To resolve two energy levels, the energy difference <math>\Delta E</math> should be greater than the sum of the two linewidths, or at least comparable to the larger linewidth. Typically, for clear resolution, <math>\Delta E \gg \Gamma_1</math> and <math>\Delta E \gg \Gamma_2</math>, but since <math>\Gamma_1</math> and <math>\Gamma_2</math> are different, we need <math>\Delta E</math> to be larger than the larger of the two widths. Let me calculate the linewidths. First, <math>\hbar = h/(2\pi)</math>, and <math>h = 4.135667662 \times 10^{-15}</math> eV·s (I think that's the value in eV seconds). I should use consistent units. Since the options are in eV, I'll work in eV. <math>\hbar</math> in eV·s is approximately <math>6.582 \times 10^{-16}</math> eV·s. Let me confirm. <math>\hbar = 4.135667662 \times 10^{-15}</math> eV·s (this is <math>h</math>, not <math>\hbar</math>) <math>\hbar = h/(2\pi) = (4.135667662 \times 10^{-15})/(6.283185307) \approx 6.582 \times 10^{-16}</math> eV·s. Yes. So <math>\hbar \approx 6.582 \times 10^{-16}</math> eV·s. Now, for state 1: <math>\tau_1 = 10^{-9}</math> s <math>\Gamma_1 = \hbar/\tau_1 = (6.582 \times 10^{-16})/(10^{-9}) = 6.582 \times 10^{-7}</math> eV. Similarly, for state 2: <math>\tau_2 = 10^{-8}</math> s <math>\Gamma_2 = \hbar/\tau_2 = (6.582 \times 10^{-16})/(10^{-8}) = 6.582 \times 10^{-8}</math> eV. So <math>\Gamma_1 \approx 6.58 \times 10^{-7}</math> eV. <math>\Gamma_2 \approx 6.58 \times 10^{-8}</math> eV. The larger linewidth is <math>\Gamma_1 \approx 6.6 \times 10^{-7}</math> eV. To clearly distinguish the two energy levels, the energy difference <math>\Delta E</math> should be much larger than the larger linewidth, so that the peaks don't overlap significantly. In the context of the question, "clearly resolve" probably means that <math>\Delta E</math> is greater than the sum of the linewidths or at least comparable to the larger one. Typically, for two lines to be resolved, the energy difference should be greater than the FWHM of the broader line. Since <math>\Gamma_1</math> is larger than <math>\Gamma_2</math>, we need <math>\Delta E &gt; \Gamma_1</math>. Let me see the options: A) <math>10^{-9}</math> eV B) <math>10^{-8}</math> eV C) <math>10^{-4}</math> eV D) <math>10^{-11}</math> eV. Now, <math>\Gamma_1 \approx 6.6 \times 10^{-7}</math> eV, which is about <math>0.66 \times 10^{-6}</math> eV. So <math>10^{-6}</math> eV is 100 times larger than <math>10^{-7}</math>, but let's compare numerically. <math>\Gamma_1 = 6.58 \times 10^{-7}</math> eV. Option A: <math>10^{-9}</math> eV = <math>0.001 \times 10^{-6}</math> eV = <math>10^{-9}</math> eV. <math>10^{-9}</math> is much smaller than <math>10^{-7}</math>, since <math>10^{-9}/10^{-7} = 10^{-2}</math>, so 100 times smaller. Option B: <math>10^{-8}</math> eV = <math>0.1 \times 10^{-7}</math> eV, still smaller than <math>\Gamma_1</math> (which is <math>\sim 6.6 \times 10^{-7}</math>, so <math>10^{-8}</math> is 10 times smaller than <math>10^{-7}</math>, but <math>\Gamma_1</math> is <math>6.6 \times 10^{-7}</math>, so <math>10^{-8}</math> is <math>0.1 \times 10^{-7} = 10^{-8}</math>, while <math>\Gamma_1</math> is <math>6.6 \times 10^{-7} = 66 \times 10^{-8}</math>, so <math>\Gamma_1</math> is about 66 times larger than <math>10^{-8}</math> eV). Let's do it properly. <math>\Gamma_1 = 6.58 \times 10^{-7}</math> eV. Option A: <math>10^{-9}</math> eV = <math>0.001 \times 10^{-6}</math> eV, but better to write in same exponent. <math>10^{-9}</math> eV vs <math>10^{-7}</math> eV: <math>10^{-9}</math> is 100 times smaller than <math>10^{-7}</math>. Specifically, <math>\Gamma_1/(10^{-9}) = 6.58 \times 10^{-7}/1 \times 10^{-9} = 658</math>, so <math>\Gamma_1</math> is 658 times larger than option A. Similarly, option B: <math>10^{-8}</math> eV. <math>\Gamma_1/(10^{-8}) = 6.58 \times 10^{-7}/1 \times 10^{-8} = 65.8</math>, so <math>\Gamma_1</math> is about 66 times larger than option B. Option C: <math>10^{-4}</math> eV. <math>\Gamma_1/(10^{-4}) = 6.58 \times 10^{-7}/1 \times 10^{-4} = 6.58 \times 10^{-3}</math>, so <math>\Gamma_1</math> is 0.00658 times <math>10^{-4}</math>, meaning <math>10^{-4}</math> is much larger than <math>\Gamma_1</math>. <math>10^{-4}</math> eV = 0.0001 eV. <math>\Gamma_1 = 0.000000658</math> eV, so yes, <math>10^{-4}</math> is 1000 times larger than <math>\Gamma_1</math>? Let's see: <math>10^{-4}/\Gamma_1 = 10^{-4}/(6.58 \times 10^{-7}) = 10^{-4}/6.58 \times 10^{-7} = (1/6.58) \times 10^3 \approx 0.152 \times 1000 = 152</math>. So <math>10^{-4}</math> eV is about 152 times larger than <math>\Gamma_1</math>. Option D: <math>10^{-11}</math> eV, which is much smaller than <math>\Gamma_1</math>.</p>

*Continued on next page*

Table 7 – *Continued from previous page*

ID	Content
5	<p>So, for clear resolution, we need <math>\Delta E</math> to be larger than <math>\Gamma_1</math>, the larger linewidth. Option C is <math>10^{-4}</math> eV, which is larger than <math>\Gamma_1</math> (since <math>\Gamma_1 \approx 10^{-6.2}</math> eV, roughly <math>6.6 \times 10^{-7}</math>, so <math>10^{-4}</math> is 1000 times larger? Wait no: <math>10^{-4} = 0.0001</math>  <math>\Gamma_1 = 0.000000658 = 6.58 \times 10^{-7}</math>  So <math>10^{-4}/\Gamma_1 = 10^{-4}/6.58 \times 10^{-7} = 1000/6.58 \approx 152</math>, so yes, about 152 times larger. Option B is <math>10^{-8}</math> eV, which is smaller than <math>\Gamma_1</math>.  <math>\Gamma_1 = 6.58 \times 10^{-7}</math>, <math>10^{-8} = 0.00000001</math>, so <math>\Gamma_1/10^{-8} = 65.8</math>, so <math>\Gamma_1</math> is 65.8 times larger than option B. Similarly, option A is even smaller. Option D is <math>10^{-11}</math>, way smaller. So only option C is larger than <math>\Gamma_1</math>. But is that sufficient? The question says "clearly distinguish these two energy levels." I think in spectroscopy, for two lines to be resolved, the energy difference should be greater than the sum of the half-widths or something. In the context of the uncertainty principle, the natural linewidth is <math>\Gamma</math>, and for two states to be distinguishable, the energy difference should be much larger than the larger linewidth. Moreover, since the states have different lifetimes, their widths are different, but the resolution criterion is often <math>\Delta E &gt; \Gamma_{\max}</math>. Let me think if there's a standard formula. Another way to think: the energy difference must be larger than the minimum resolvable difference. The uncertainty principle gives the intrinsic width, so if <math>\Delta E</math> is smaller than <math>\Gamma_1</math>, the two levels would be indistinguishable because the width of the first state is <math>\Gamma_1</math>, so it's spread over an energy range of about <math>\Gamma_1</math>, so if the difference is less than <math>\Gamma_1</math>, it might be within the spread. Specifically, for the two levels to be resolved, we need <math> E_1 - E_2  &gt; \Gamma_1</math> and <math> E_1 - E_2  &gt; \Gamma_2</math>, but since <math>\Gamma_1 &gt; \Gamma_2</math>, it's sufficient to have <math> E_1 - E_2  &gt; \Gamma_1</math>. In this case, <math>\Gamma_1</math> is about <math>6.6 \times 10^{-7}</math> eV, so we need <math>\Delta E &gt; 6.6 \times 10^{-7}</math> eV. Option C is <math>10^{-4}</math> eV = <math>0.0001</math> eV = <math>1 \times 10^{-4}</math> eV, which is 100 times larger than <math>1 \times 10^{-6}</math>? <math>1 \times 10^{-4} = 100,000 \times 10^{-9}</math>, but <math>\Gamma_1 = 6.6 \times 10^{-7} = 0.66 \times 10^{-6}</math>. <math>1 \times 10^{-4} = 100 \times 10^{-6}</math>, <math>\Gamma_1 = 0.66 \times 10^{-6}</math>, so yes, <math>100 \times 10^{-6}/0.66 \times 10^{-6} \approx 151.5</math>, so about 150 times larger. Option B is <math>1 \times 10^{-8}</math> eV, which is <math>0.01 \times 10^{-6}</math>, while <math>\Gamma_1</math> is <math>0.66 \times 10^{-6}</math>, so <math>\Gamma_1</math> is about 66 times larger than option B. So if <math>\Delta E</math> is <math>10^{-8}</math> eV, it's smaller than <math>\Gamma_1</math>, so the two peaks would overlap significantly. Similarly, for option C, it's larger, so they should be resolved. But let me check the options again. Option C is <math>10^{-4}</math> eV, which is 0.0001 eV. Is there a trick here? The question says: "we want to clearly distinguish these two energy levels." And the states have energies <math>E_1</math> and <math>E_2</math>, with lifetimes given. But in quantum mechanics, the energy levels themselves might be degenerate or something, but I think here it's about the transition energies or something? No, it says "energy levels" with energies <math>E_1</math> and <math>E_2</math>. Perhaps it's about the energy difference between them. Another thought: in the context of the uncertainty principle, the energy difference must be such that it's not affected by the broadening. I recall that for two states to be resolved, the energy difference should be greater than the sum of the decay widths. The sum <math>\Gamma_1 + \Gamma_2 \approx 6.58 \times 10^{-7} + 6.58 \times 10^{-8} = 7.24 \times 10^{-7}</math> eV. Still, option C is <math>1 \times 10^{-4}</math>, which is much larger. Option B is <math>1 \times 10^{-8}</math>, which is less than both. But let's see the answer choices; D is <math>10^{-11}</math>, which is tiny. Perhaps I misremembered the uncertainty principle. Is it <math>\Delta E \cdot \tau = \hbar</math> or <math>\hbar/2</math>? In many contexts, the natural linewidth is <math>\Gamma = \hbar/\tau</math>, so for a state with lifetime <math>\tau</math>, the energy uncertainty is <math>\hbar/\tau</math>. Yes. Sometimes it's given as the full width at half maximum (FWHM) is <math>\Gamma = \hbar/\tau</math>. So I think that's standard. Perhaps the question is about the energy difference for the transition, but it says "energy levels" with energies <math>E_1</math> and <math>E_2</math>.</p>

*Continued on next page*

Table 7 – *Continued from previous page*

ID	Content
5	<p>Another angle: if the two energy levels are close, they might mix, but I think for resolution, it's about the width.</p> <p>Let me see if there's a specific formula for resolution.</p> <p>In spectroscopy, the Rayleigh criterion for resolution is that the energy difference should be greater than the FWHM of the broader line.</p> <p>Here, the broader line has <math>\Gamma_1 = \hbar/\tau_1 = \hbar/10^{-9}</math></p> <p>Since <math>\tau_1 &lt; \tau_2</math>, <math>\Gamma_1 &gt; \Gamma_2</math>, so <math>\Gamma_1</math> is larger.</p> <p>So <math>\Delta E &gt; \Gamma_1</math> for clear resolution.</p> <p><math>\Gamma_1 = \hbar/\tau_1</math></p> <p><math>\hbar \approx 6.58 \times 10^{-16} \text{ eV}\cdot\text{s}</math></p> <p><math>\tau_1 = 1 \times 10^{-9} \text{ s}</math></p> <p><math>\Gamma_1 = 6.58 \times 10^{-16}/1 \times 10^{-9} = 6.58 \times 10^{-7} \text{ eV}</math></p> <p>Now, options:</p> <p>A) <math>1 \times 10^{-9} \text{ eV} \rightarrow</math> too small</p> <p>B) <math>1 \times 10^{-8} \text{ eV} \rightarrow 1 \times 10^{-8} &lt; 6.58 \times 10^{-7}</math>? <math>1 \times 10^{-8} = 0.1 \times 10^{-7}</math>, <math>6.58 \times 10^{-7} = 65.8 \times 10^{-8}</math>, so <math>65.8 \times 10^{-8} &gt; 1 \times 10^{-8}</math>, yes, so smaller</p> <p>C) <math>1 \times 10^{-4} \text{ eV} = 100 \times 10^{-6} \text{ eV}</math>, while <math>\Gamma_1 = 0.658 \times 10^{-6} \text{ eV}</math>, so <math>100 \times 10^{-6} &gt; 0.658 \times 10^{-6}</math>, yes</p> <p>D) <math>1 \times 10^{-11} \text{ eV} \rightarrow</math> way smaller</p> <p>So only C is larger than <math>\Gamma_1</math>.</p> <p>But let me check if the question is tricky.</p> <p>The lifetimes are for the states, but when we say "distinguish these two energy levels", it might be in a measurement context.</p> <p>Perhaps the energy difference must be such that the time it takes to resolve is related.</p> <p>Another thought: the minimum resolvable energy difference is on the order of <math>\hbar/\tau</math>, but for two states, it might be different.</p> <p>I recall that in the context of the uncertainty principle, the energy difference <math>\Delta E</math> must satisfy <math>\Delta E &gt; \hbar/\tau</math> for some <math>\tau</math>, but here we have two different <math>\tau</math>.</p> <p>I think my initial approach is correct.</p> <p>Let me calculate numerically.</p> <p><math>\hbar = 1.0545718 \times 10^{-34} \text{ J}\cdot\text{s}</math></p> <p>But in eV, <math>\hbar = 6.582 \times 10^{-16} \text{ eV}\cdot\text{s}</math>, as I had.</p> <p><math>\tau_1 = 10^{-9} \text{ s}</math></p> <p><math>\Gamma_1 = \hbar/\tau_1 = 6.582 \times 10^{-16}/1 \times 10^{-9} = 6.582 \times 10^{-7} \text{ eV}</math></p> <p>Similarly, <math>\tau_2 = 10^{-8} \text{ s}</math>, <math>\Gamma_2 = 6.582 \times 10^{-16}/1 \times 10^{-8} = 6.582 \times 10^{-8} \text{ eV}</math></p> <p>So <math>\Gamma_{\max} = \Gamma_1 = 6.582 \times 10^{-7} \text{ eV}</math></p> <p>For clear resolution, <math>\Delta E</math> should be greater than, say, 10 times <math>\Gamma_{\max}</math> or something? But typically, if it's a factor of 2 or 3, it might be barely resolved, but for "clearly distinguish", it should be significantly larger.</p> <p>In multiple choice, option C is <math>10^{-4} \text{ eV}</math>, which is about 150 times larger than <math>\Gamma_1</math>.</p> <p>Option B is <math>10^{-8} \text{ eV}</math>, which is about 66 times smaller than <math>\Gamma_1</math>.</p> <p>So if <math>\Delta E = 10^{-8} \text{ eV}</math>, and <math>\Gamma_1 = 6.58 \times 10^{-7} \text{ eV}</math>, then the relative difference is <math>(10^{-8})/(6.58 \times 10^{-7}) \approx 0.015</math>, so 1.5</p> <p>Whereas for C, it's 150 times larger, so very clear.</p> <p>Option D is even smaller.</p> <p>But is there a possibility that I have the uncertainty principle wrong?</p> <p>Sometimes people use the time-energy uncertainty as <math>\Delta E \Delta t \geq \hbar/2</math>, so the minimum uncertainty is <math>\hbar/2</math>, but for lifetime, it's often approximated as <math>\Delta E \approx \hbar/\tau</math>.</p> <p>In many textbooks, for the natural linewidth, <math>\Gamma = \hbar/\tau</math>.</p> <p>For example, in the context of the uncertainty principle for decay, the energy width is <math>\hbar/\tau</math>.</p> <p>So I think it's correct.</p> <p>Perhaps the question is about the energy difference for the transition between them, but it says "energy levels" with energies <math>E_1</math> and <math>E_2</math>.</p> <p>Another interpretation: if the two energy levels are close, they might not be distinct because of broadening.</p> <p>But the question is: "we want to clearly distinguish these two energy levels" meaning that we want to see them as separate lines.</p> <p>So yes, the energy difference must be larger than the linewidths.</p> <p>Moreover, looking at the options, D is <math>10^{-11} \text{ eV}</math>, which is extremely small, while the lifetimes are given in seconds, so it should be larger.</p> <p>Let me see the answer choices; C is <math>10^{-4} \text{ eV}</math>, which seems reasonable.</p> <p>But let me see if there's a calculation mistake.</p>

*Continued on next page*

Table 7 – *Continued from previous page*

ID	Content
5	<p><math>\tau_1 = 10^{-9}</math> s, so <math>\Gamma_1 = \hbar/\tau_1</math>  <math>\hbar</math> in eV·s is about <math>6.58 \times 10^{-16}</math>  <math>\Gamma_1 = 6.58 \times 10^{-16}/1 \times 10^{-9} = 6.58 \times 10^{-7}</math> eV  <math>10^{-7}</math> eV is 0.0000001 eV, <math>\Gamma_1</math> is 0.000000658 eV.      Option B is <math>10^{-8}</math> eV = 0.00000001 eV, which is smaller.      Option C is <math>10^{-4}</math> eV = 0.0001 eV.      Yes.      Perhaps the question is about the energy difference in terms of the uncertainty.      Another thought: in some contexts, for two states to be distinguishable, the energy difference should be greater than the uncertainty of each, but since they have different uncertainties, we take the larger one.      I think C is correct.      But let me see why the other options might be tempting.      Option D is <math>10^{-11}</math> eV, which is smaller than <math>\Gamma_1</math> by a factor of about 60,000, so no.      Option A is <math>10^{-9}</math>, even smaller.      Option B is <math>10^{-8}</math>, which is close to <math>\Gamma_2</math> but smaller than <math>\Gamma_1</math>.  <math>\Gamma_2</math> is <math>6.58 \times 10^{-8}</math>, so <math>10^{-8}</math> is about 0.658 times <math>\Gamma_2</math>? <math>10^{-8}/6.58 \times 10^{-8} \approx 0.152</math>, so about 15      Whereas for C, it's large.      Perhaps the question is misstated, but I think C is the answer.      I recall that in some multiple-choice questions, they use the formula directly.      For example, the energy difference must be at least on the order of <math>\hbar/\tau</math>, and since <math>\tau</math> is <math>10^{-9}</math> s for the first state, <math>\hbar/\tau \approx 10^{-6}</math> eV or something.  <math>\hbar/\tau_1 = 6.58 \times 10^{-7}</math> eV, which is about <math>10^{-6}</math> eV (since <math>10^{-6}</math> is <math>1 \times 10^{-6}</math>, <math>6.58 \times 10^{-7}</math> is <math>0.658 \times 10^{-6}</math>).      Options: A is <math>10^{-9}</math>, B <math>10^{-8}</math>, C <math>10^{-4}</math>, D <math>10^{-11}</math>  <math>10^{-4}</math> is 100 times larger than <math>10^{-6}</math>, so it's fine.  <math>10^{-8}</math> is 100 times smaller than <math>10^{-6}</math>.      So yes.      Perhaps they expect us to compute <math>\hbar/\tau</math> for the shorter lifetime.      The shortest lifetime is <math>\tau_1 = 10^{-9}</math> s, so <math>\Gamma_1</math> is largest.      So <math>\Delta E &gt; \hbar/\tau_1</math>      Now, <math>\hbar/\tau_1 \approx 6.6 \times 10^{-7}</math> eV      Which is closest to <math>10^{-6}</math> eV, but the options don't have <math>10^{-6}</math>, they have <math>10^{-4}</math> and <math>10^{-8}</math>.  <math>10^{-4}</math> is 100 times larger, but it's the only one larger.  <math>10^{-8}</math> is smaller.      So in multiple choice, C is the only one that is larger.      Option B is <math>10^{-8}</math>, which is smaller than <math>\Gamma_1</math>.      Unless I miscalculated <math>\hbar</math>.      Let me double-check <math>\hbar</math> in eV·s.  <math>h = 4.135667662 \times 10^{-15}</math> eV·s (Planck's constant)  <math>\hbar = h/(2\pi) = 4.135667662 \times 10^{-15}/6.283185307 \approx?</math>  <math>4.135667662 \times 10^{-15}/6.283185307 \approx (4.135667662/6.283185307) \times 10^{-15} \approx 0.6582 \times 10^{-15} = 6.582 \times 10^{-16}</math> eV·s. Yes.  <math>\tau_1 = 10^{-9}</math> s  <math>\Gamma_1 = 6.582 \times 10^{-16}/1 \times 10^{-9} = 6.582 \times 10^{-7}</math> eV      Yes.  <math>10^{-7}</math> eV is 0.0000001 eV, <math>\Gamma_1</math> is 0.0000006582 eV.      Option C: <math>10^{-4} = 0.0001</math> eV, which is 1000 times larger? <math>0.0001/0.0000006582 \approx 152</math>, so about 150 times.      In spectroscopy, for two lines to be resolved, the energy difference should be greater than the FWHM of the broader line, which is <math>\Gamma_1</math> here.      So C should be correct.      Perhaps the question is about the energy difference for the transition, but it says "energy levels" with energies <math>E_1</math> and <math>E_2</math>.      Another interpretation: if the two energy levels are degenerate or something, but I think not.      Perhaps "clearly distinguish" means that the energy difference is much larger than the uncertainty.      I think I'm overcomplicating.      Let me see the answer choices; D is <math>10^{-11}</math> eV, which is way too small.      For example, if <math>\Delta E</math> were <math>10^{-11}</math> eV, and <math>\Gamma_1</math> is <math>10^{-6}</math> eV, then <math>\Delta E</math> is 100,000 times smaller, so completely unresolved.</p>

*Continued on next page*

Table 7 – *Continued from previous page*

ID	Content
5	<p>Similarly, <math>B</math> is <math>10^{-8}</math>, which is 60 times smaller than <math>\Gamma_1</math>.  <math>C</math> is 150 times larger.  So <math>C</math> is the only reasonable choice.  Perhaps they want the difference to be at least <math>\hbar/(\tau_1 + \tau_2)</math> or something, but that doesn't make sense.  Or the minimum resolvable difference is <math>\hbar/\tau</math> for the shortest lifetime.  I think <math>C</math> is correct.  So I'll go with <math>C</math>.  But let me see the options again.  A) <math>10^{-9}</math> eV  B) <math>10^{-8}</math> eV  C) <math>10^{-4}</math> eV  D) <math>10^{-11}</math> eV  Yes.  In some contexts, for time-energy, but I think it's fine.  So the answer should be <math>C</math>.  The question says "which one of the following options could be their energy difference so that they can be clearly resolved?"  And <math>C</math> is <math>10^{-4}</math> eV.  Perhaps they expect a calculation without numbers.  For example, <math>\Gamma_1 \approx \hbar/\tau_1</math>, <math>\tau_1 = 10^{-9}</math> s  <math>\hbar \approx 10^{-15}</math> eV·s (roughly, since <math>6.58 \times 10^{-16}</math> is about <math>10^{-15}</math>)  So <math>\Gamma_1 \approx 10^{-15}/10^{-9} = 10^{-6}</math> eV  Similarly, <math>\Gamma_2 \approx 10^{-15}/10^{-8} = 10^{-7}</math> eV  So <math>\Gamma_{\max} \approx 10^{-6}</math> eV  Then <math>\Delta E &gt; 10^{-6}</math> eV for clear resolution.  Options: A <math>10^{-9}</math>, B <math>10^{-8}</math>, C <math>10^{-4}</math>, D <math>10^{-11}</math>  <math>10^{-4}</math> is 100 times larger than <math>10^{-6}</math>, so it works.  <math>10^{-8}</math> is 100 times smaller than <math>10^{-6}</math>.  So yes.  Therefore, the answer is <math>C</math>.  I think that's it.  To determine which energy difference allows clear distinction between two quantum states with lifetimes of <math>10^{-9}</math> seconds and <math>10^{-8}</math> seconds, the energy uncertainty due to the finite lifetime must be considered.  According to the Heisenberg uncertainty principle, the energy uncertainty <math>\Delta E</math> for a state with lifetime <math>\tau</math> is approximately <math>\Delta E \approx \hbar/\tau</math>, where <math>\hbar</math> is the reduced Planck's constant (<math>\hbar \approx 6.582 \times 10^{-16}</math> eV · s).  For the state with lifetime <math>\tau_1 = 10^{-9}</math> s:  <math display="block">\Gamma_1 = \frac{\hbar}{\tau_1} = \frac{6.582 \times 10^{-16}}{10^{-9}} = 6.582 \times 10^{-7}</math> eV  For the state with lifetime <math>\tau_2 = 10^{-8}</math> s:  <math display="block">\Gamma_2 = \frac{\hbar}{\tau_2} = \frac{6.582 \times 10^{-16}}{10^{-8}} = 6.582 \times 10^{-8}</math> eV  The larger energy uncertainty is <math>\Gamma_1 \approx 6.582 \times 10^{-7}</math> eV. To clearly resolve two energy levels, the energy difference <math>\Delta E</math> must be significantly larger than the larger uncertainty <math>\Gamma_1</math> (typically by a factor of at least 10-100 for clear distinction).  Now, evaluate the options: - A) <math>10^{-9}</math> eV: <math>10^{-9}/6.582 \times 10^{-7} \approx 0.0015</math>, so <math>\Delta E</math> is about 0.15- B) <math>10^{-8}</math> eV: <math>10^{-8}/6.582 \times 10^{-7} \approx 0.015</math>, so <math>\Delta E</math> is about 1.5- C) <math>10^{-4}</math> eV: <math>10^{-4}/6.582 \times 10^{-7} \approx 152</math>, so <math>\Delta E</math> is about 152 times larger than <math>\Gamma_1</math>—sufficient for clear resolution. - D) <math>10^{-11}</math> eV: <math>10^{-11}/6.582 \times 10^{-7} \approx 0.000015</math>, so <math>\Delta E</math> is about 0.0015  Only option C satisfies the condition for clear resolution, as it is much larger than the larger energy uncertainty <math>\Gamma_1</math>.  ANSWER: C</p>

Table 8: Detailed individual metrics for different merging granularities (full data).

ID	Method	f1 (↑)	f2 (↑)	GPQA_ACC (↑)	GPQA_TOKENS (↓)	AIME25_ACC (↑)	AIME25_TOKENS (↓)	Pareto
0	Layer-wise	0.8698	0.8047	0.6212	4037	0.7666	8891	✓
1		0.9527	0.2414	0.6616	9136	0.7666	15496	✗
2		0.3656	1.0585	0.4545	791	0.6666	7321	✓
3		0.6848	0.8697	0.6364	3427	0.6333	8161	✓
4		0.3428	1.0599	0.4697	958	0.6333	7037	✓
5		0.1783	1.0666	0.4949	764	0.5000	7158	✓
6		0.2116	1.0600	0.4848	717	0.5333	7392	✓
7		0.8826	0.7393	0.6010	4308	0.8000	10132	✓
8		0.5753	1.0409	0.5303	900	0.7000	7602	✓
9		0.6101	0.9011	0.6263	2509	0.6000	8732	✓
0	Block-wise (n=18)	1.0691	0.5632	0.6919	6660	0.8000	11077	✓
1		0.6894	0.7855	0.5859	4706	0.7000	8384	✗
2		0.5086	1.0210	0.5505	1573	0.6333	7106	✗
3		0.7308	0.7012	0.6061	5104	0.7000	9912	✗
4		0.1266	1.0383	0.4697	981	0.5000	7545	✗
5		0.5455	0.9135	0.6212	2698	0.5666	8140	✗
6		0.8677	0.6257	0.6465	6076	0.7333	10369	✗
7		0.7183	0.7383	0.6263	3923	0.6667	10729	✗
8		0.8552	0.6671	0.6667	5376	0.7000	10366	✗
0	Block-wise (n=9)	0.9320	0.4935	0.6515	7576	0.7666	11472	✗
1		0.9735	0.3001	0.6717	8549	0.7666	14888	✗
2		0.8552	0.5161	0.6667	7219	0.7000	11430	✗
3		0.7411	0.6215	0.6111	6391	0.7000	10008	✗
4		0.5628	0.8946	0.5505	1273	0.6667	10726	✗
5		0.6284	0.8021	0.6616	4832	0.5666	7779	✗
6		0.4776	0.9933	0.5354	1680	0.6333	7643	✗
7		1.0611	0.2645	0.6616	8242	0.8334	16240	✗
8		0.7930	0.6184	0.6364	6471	0.7000	9968	✗
9	Model-level	1.0818	0.2037	0.6717	8082	0.8334	18005	✗
10		0.3822	1.0249	0.5152	1226	0.6000	7520	✗
11		1.0715	0.2445	0.6667	8176	0.8334	16841	✗
12		1.0506	0.2790	0.6566	8406	0.8333	15631	✗
13		0.9506	0.3431	0.6869	8263	0.7333	14233	✗
0		0.4983	0.9734	0.5455	1441	0.6333	8496	✗
1		0.5168	0.9129	0.5808	3197	0.6000	7417	✗
2		0.5227	0.7743	0.6364	4966	0.5333	8279	✗
3		0.6516	0.6855	0.6465	6165	0.6000	8735	✗
4		0.5812	0.7023	0.5859	6368	0.6333	8013	✗
5		0.7700	0.6019	0.6515	7065	0.6667	9503	✗
6		0.8012	0.5726	0.6667	7220	0.6667	10008	✗
7		0.8885	0.5154	0.6566	7697	0.7333	10740	✗
8		0.8906	0.3548	0.6313	8851	0.7666	13067	✗
9	GPQA-Diamond	1.0691	0.3285	0.6919	8812	0.8000	13786	✗
10		1.0923	0.3010	0.6768	8571	0.8334	14834	✓
11		1.1231	0.2153	0.6919	8443	0.8333	17178	✓
12		1.1438	0.2042	0.7020	8560	0.8333	17285	✓

<sup>1</sup> Metrics evaluated on the GPQA-Diamond dataset.

<sup>2</sup> Metrics evaluated on the AIME25 dataset.